

# Towards a Smart World: Hazard Levels for Monitoring of Autonomous Vehicles' Swarms

Francesca M. Favaro, PhD  
Shivangi Agarwal  
Nazanin Nader  
Sumaid Mahmood



# MINETA TRANSPORTATION INSTITUTE

## LEAD UNIVERSITY OF

### Mineta Consortium for Transportation Mobility

Founded in 1991, the Mineta Transportation Institute (MTI), an organized research and training unit in partnership with the Lucas College and Graduate School of Business at San José State University (SJSU), increases mobility for all by improving the safety, efficiency, accessibility, and convenience of our nation's transportation system. Through research, education, workforce development, and technology transfer, we help create a connected world. MTI leads the four-university Mineta Consortium for Transportation Mobility, a Tier I University Transportation Center funded by the U.S. Department of Transportation's Office of the Assistant Secretary for Research and Technology (OST-R), the California Department of Transportation (Caltrans), and by private grants and donations.

MTI's transportation policy work is centered on three primary responsibilities:

#### Research

MTI works to provide policy-oriented research for all levels of government and the private sector to foster the development of optimum surface transportation systems. Research areas include: bicycle and pedestrian issues; financing public and private sector transportation improvements; intermodal connectivity and integration; safety and security of transportation systems; sustainability of transportation systems; transportation / land use / environment; and transportation planning and policy development. Certified Research Associates conduct the research. Certification requires an advanced degree, generally a PhD, a record of academic publications, and professional references. Research projects culminate in a peer-reviewed publication, available on TransWeb, the MTI website (<http://transweb.sjsu.edu>).

#### Education

The Institute supports education programs for students seeking a career in the development and operation of surface transportation systems. MTI, through San José State University, offers an AACSB-accredited Master of Science in Transportation Management and graduate certificates in Transportation Management, Transportation Security, and High-Speed Rail Management that serve to prepare the nation's transportation managers for the 21st century. With the

active assistance of the California Department of Transportation (Caltrans), MTI delivers its classes over a state-of-the-art videoconference network throughout the state of California and via webcasting beyond, allowing working transportation professionals to pursue an advanced degree regardless of their location. To meet the needs of employers seeking a diverse workforce, MTI's education program promotes enrollment to under-represented groups.

#### Information and Technology Transfer

MTI utilizes a diverse array of dissemination methods and media to ensure research results reach those responsible for managing change. These methods include publication, seminars, workshops, websites, social media, webinars, and other technology transfer mechanisms. Additionally, MTI promotes the availability of completed research to professional organizations and journals and works to integrate the research findings into the graduate education program. MTI's extensive collection of transportation-related publications is integrated into San José State University's world-class Martin Luther King, Jr. Library.

---

#### Disclaimer

The contents of this report reflect the views of the authors, who are responsible for the facts and accuracy of the information presented herein. This document is disseminated in the interest of information exchange. The report is funded, partially or entirely, by a grant from the U.S. Department of Transportation's University Transportation Centers Program. This report does not necessarily reflect the official views or policies of the U.S. government, State of California, or the Mineta Transportation Institute, who assume no liability for the contents or use thereof. This report does not constitute a standard specification, design standard, or regulation.

REPORT WP 18-07

**TOWARDS A SMART WORLD:  
HAZARD LEVELS FOR MONITORING OF  
AUTONOMOUS VEHICLES' SWARMS**

Francesca M. Favaro, PhD  
Shivangi Agarwal  
Nazanin Nader  
Sumaid Mahmood

August 2018

A publication of

**Mineta Transportation Institute**

Created by Congress in 1991

College of Business  
San José State University  
San José, CA 95192-0219

# TECHNICAL REPORT DOCUMENTATION PAGE

<b>1. Report No.</b> WP 18-07	<b>2. Government Accession No.</b>	<b>3. Recipient's Catalog No.</b>	
<b>4. Title and Subtitle</b> Towards a Smart World: Hazard Levels for Monitoring of Autonomous Vehicles' Swarms		<b>5. Report Date</b> August 2018	
		<b>6. Performing Organization Code</b>	
<b>7. Authors</b> Francesca Favaro, PhD, <a href="https://orcid.org/0000-0003-0239-0770">https://orcid.org/0000-0003-0239-0770</a> Shivangi Agarwal, <a href="https://orcid.org/0000-0001-8765-432X">https://orcid.org/0000-0001-8765-432X</a> Nazanin Nader, <a href="https://orcid.org/0000-0002-1159-4591">https://orcid.org/0000-0002-1159-4591</a> Sumaid Mahmood, <a href="https://orcid.org/0000-0003-1127-8836">https://orcid.org/0000-0003-1127-8836</a>		<b>8. Performing Organization Report</b> CA-MTI-1735	
<b>9. Performing Organization Name and Address</b> Mineta Transportation Institute College of Business San José State University San José, CA 95192-0219		<b>10. Work Unit No.</b>	
		<b>11. Contract or Grant No.</b> 69A3551747127	
<b>12. Sponsoring Agency Name and Address</b> U.S. Department of Transportation Office of the Assistant Secretary for Research and Technology University Transportation Centers Program 1200 New Jersey Avenue, SE Washington, DC 20590		<b>13. Type of Report and Period Covered</b> Final Report	
		<b>14. Sponsoring Agency Code</b>	
<b>15. Supplemental Notes</b>			
<b>16. Abstract</b> <p>This work explores the creation of quantifiable indices to monitor the safe operations and movement of families of autonomous vehicles (AV) in restricted highway-like environments. Specifically, this work will explore the creation of ad-hoc rules for monitoring lateral and longitudinal movement of multiple AVs based on behavior that mimics swarm and flock movement (or particle swarm motion).</p> <p>This exploratory work is sponsored by the Emerging Leader Seed grant program of the Mineta Transportation Institute and aims at investigating feasibility of adaptation of particle swarm motion to control families of autonomous vehicles. Specifically, it explores how particle swarm approaches can be augmented by setting safety thresholds and fail-safe mechanisms to avoid collisions in off-nominal situations. This concept leverages the integration of the notion of hazard and danger levels (i.e., measures of the "closeness" to a given accident scenario, typically used in robotics) with the concept of safety distance and separation/collision avoidance for ground vehicles. A draft of implementation of four hazard level functions indicates that safety thresholds can be set up to autonomously trigger lateral and longitudinal motion control based on three main rules respectively based on speed, heading, and breaking distance to steer the vehicle and maintain separation/avoid collisions in families of autonomous vehicles. The concepts here presented can be used to set up a high-level framework for developing artificial intelligence algorithms that can serve as back-up to standard machine learning approaches for control and steering of autonomous vehicles. Although there are no constraints on the concept's implementation, it is expected that this work would be most relevant for highly-automated Level 4 and Level 5 vehicles, capable of communicating with each other and in the presence of a monitoring ground control center for the operations of the swarm.</p>			
<b>17. Key Words</b> Autonomous vehicles; vehicles swarm; hazard monitoring; collision avoidance; safety thresholds		<b>18. Distribution Statement</b> No restrictions. This document is available to the public through The National Technical Information Service, Springfield, VA 22161	
<b>19. Security Classif. (of this report)</b> Unclassified	<b>20. Security Classif. (of this page)</b> Unclassified	<b>21. No. of Pages</b> 37	<b>22. Price</b> \$15.00

Copyright © 2018  
by **Mineta Transportation Institute**  
All rights reserved

Library of Congress Catalog Card Number:  
2018953130

**To order this publication, please contact:**

Mineta Transportation Institute  
College of Business  
San José State University  
San José, CA 95192-0219

Tel: (408) 924-7560  
Fax: (408) 924-7565  
Email: [mineta-institute@sjsu.edu](mailto:mineta-institute@sjsu.edu)

[transweb.sjsu.edu](http://transweb.sjsu.edu)

## **ACKNOWLEDGMENTS**

The present work was funded through the Emerging Leader Seed Grant Program offered by the Mineta Transportation Institute (MTI) of San Jose, CA. The authors would like to thank MTI Executive Director Dr. Karen Philbrick, as well as Dr. Hilary Nixon – Director of Research and Technology Transfer for all the help and support during the proposal submission and study. The authors would also like to thank all MTI staff that assisted during the duration of the project.

The contents of this report reflect the views of the authors, who are responsible for the facts and accuracy of the information presented herein. This report does not necessarily reflect the official views or policies of the U.S. government, State of California, or the Mineta Transportation Institute, who assume no liability for the contents or use thereof. This report does not constitute a standard specification, design standard, or regulation.

---

## TABLE OF CONTENTS

<b>I. Introduction</b>	<b>1</b>
The General Idea	1
Scope of the Work	2
<b>II. An Overview of Particle Swarm</b>	<b>4</b>
The Original Use: Particle Swarm Optimization and Rules for Minimum Finding	4
Adapting PSO to Vehicles Control	5
<b>III. Swarm Motion Implementation and Hazard-Level Monitoring</b>	<b>10</b>
The Notion of Dynamic Cluster	10
The Notion of Hazard Level	13
Creating Safety Tresholds for Separation Control Based on the Three Particle Swarm Rules	15
<b>IV. Conclusions</b>	<b>29</b>
Putting It All Together	29
Future Work and Extensions	30
<b>Acronyms and Abbreviations</b>	<b>32</b>
<b>Bibliography</b>	<b>33</b>
<b>Peer Review</b>	<b>36</b>

---

## LIST OF FIGURES

1. Examples of Swarm Movements Observed in Nature	1
2. Schematic Representation of Adaptive Cruise Control Function	2
3. Schematic Representation of a “Multi-Body” Swarm-Type Control	3
4. Visual Representation of the Minimum-Finding Original PSO Algorithm for a Sample Nonlinear Function	4
5. The Three Swarm Rules Identified by Reynolds (1987) and Suggestion for the “Particle” Motion According to PSO	5
6. Possible Principal Directions of Movement in a 2-D Context	6
7. Coordinates Used to Identify Vehicle Location and Heading	6
8. Generic Representation of Collision Avoidance	7
9. Generic Representation of Weighted Heading Selection	7
10. Schematic Representation of the Velocity Matching Concept	8
11. Flow Diagram for Cluster Definition Based on Distance and Maximum Size	11
12. Cluster with Eight Neighboring Spots Filled. Here the Radius of 286 ft. Gives a Swarm Width of 572 ft.	12
13. Hazard Level Dynamical Behavior in Time	13
14. Example Hazard Level Dynamics for $H(T) = V(T)/V_{safe}$	15
15. Representation and Notation used for the Case of Two Vehicles (A and B) Travelling Longitudinally	17
16. Contour Levels for $H(T)$ as a Function of Initial Speed and Relative Distance (Dry Road)	18
17. Contour Levels for $H(T)$ as a Function of Initial Speed and Relative Distance (Icy Road)	19
18. Contour Levels for $H(T)$ Based on Stopping Distance of Vehicle in Back When Both Vehicles Moving	20
19. Conceptual Representation of the Safety Radii for Vehicles of Different Dimensions	20

---

20. Contour Levels for the 2-D Hazard Level Based on Spheres of Influence	21
21. Example of Heading Selection for a Middle Vehicle Based on Two Surrounding Vehicles' Information	22
22. Angular Error Definition	24
23. Lateral Error Definition	24
24. Generic Situation Which Combines both Lateral and Angular Error	25
25. Contour Levels for the Angular and Lateral Error Hazard Function	26
26. Schematic Representation of a Vehicle Entering a Swarm	27
27. Speed Matching Hazard Level for Vehicle Entering a Swarm	28
28. Flow Diagram for the Application of the Proposed Concepts	30

## LIST OF TABLES

1. Summary of the Developed Functions	29
---------------------------------------	----

# I. INTRODUCTION

## THE GENERAL IDEA

We are witnessing a rapid increase in the deployment of Autonomous Vehicles (AVs) on public roads. The quick spread of this technology has led many researchers to look into novel and innovative ways to model the interaction of multiple vehicles (Chater et al., 2018; Bidoki, Mortasavi, and Sabzehparvar, 2018; Åsljung, Nilsson, and Fredriksson, 2017; Barnes, Fields, and Valavanis, 2007). One such unconventional approach to solving the problem of controlling multiple AVs at the same time stems from an analogy with the behavior of swarms and flocks in nature. In technical jargon, this specific type of motion is referred to as “particle swarm motion.”

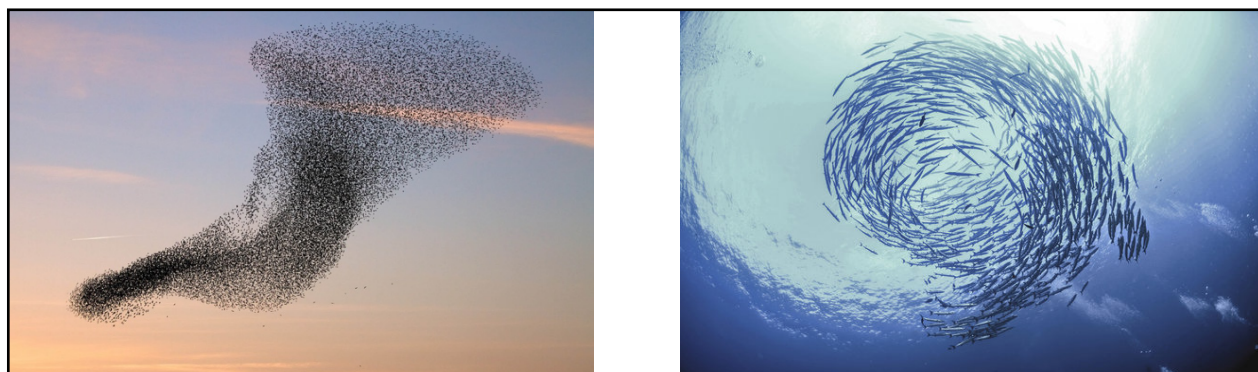


**Figure 1. Examples of Swarm Movements Observed in Nature**

Source: (left) <https://www.youtube.com/watch?v=08v446aEj-0> (right) [https://www.google.it/search?sa=G&hl=en-IT&q=school+of+herring+fish&tbs=isch&tbs=simg:CAQSmQEJa8uxqFwkeOYajQELEKjU2AQaBggVCAEICQwLELCMpwgaYgpgCAMSKK8D6RWZC60DmAv3FswBrAPJAZYLojfgKK83tTfpKLY34iirN7A3tzcaMF9Ff7SL0JeTv5VmDfsOCHid25iib4c-kE5t9Du282-\\_1h](https://www.google.it/search?sa=G&hl=en-IT&q=school+of+herring+fish&tbs=isch&tbs=simg:CAQSmQEJa8uxqFwkeOYajQELEKjU2AQaBggVCAEICQwLELCMpwgaYgpgCAMSKK8D6RWZC60DmAv3FswBrAPJAZYLojfgKK83tTfpKLY34iirN7A3tzcaMF9Ff7SL0JeTv5VmDfsOCHid25iib4c-kE5t9Du282-_1h)

Particle swarm motion has been investigated in the past as a meta-heuristic model for optimization problems. In the field of mathematics and optimization, particle swarm algorithms allow identification of the minimum or maximum of an objective function by iteratively analyzing the movement of multiple particles that abide by strict rules which model the natural behaviors of coordinated collective families of animals (like birds or fish as in Figure 1). The rules originally proposed ensure that each particle of the swarm maintains separation, alignment, and cohesion with all the other particles (Kennedy and Eberhart, 1995; Reynolds, 1987). These rules have been adapted to model and simulate the coordinated movement of both animated and inanimate objects (e.g., drone motion or crowds modeling (Corner and Lamont, 2004; Moussaid et al., 2009) and can be adapted to families of autonomous vehicles in limited-access roads (Liu, Passino, and Polycarpou, 2003; Suzuki and Yamashita, 1999; Fredette and Özgüner, 2017), where drivers are no longer needed as the vehicle movement becomes controlled by the particle swarm rules.

## SCOPE OF THE WORK

This work will explore the creation of ad-hoc indices for monitoring the motion of swarms of AVs and quantify the associated safety of operations. Safety thresholds, which will help discern whether a given vehicle is operating within its safety operational region or not, will be devised based on the rules of particle swarm motion. In a way, the adoption of particle swarm motion for ground vehicles can be thought of as an extension/generalization of what systems like adaptive cruise control currently do. Adaptive cruise control (ACC) detects the relative position and speed of a lead vehicle and adjusts the vehicle's own speed to maintain separation (i.e., avoid a collision). A typical representation of this notion is shown in Figure 2.

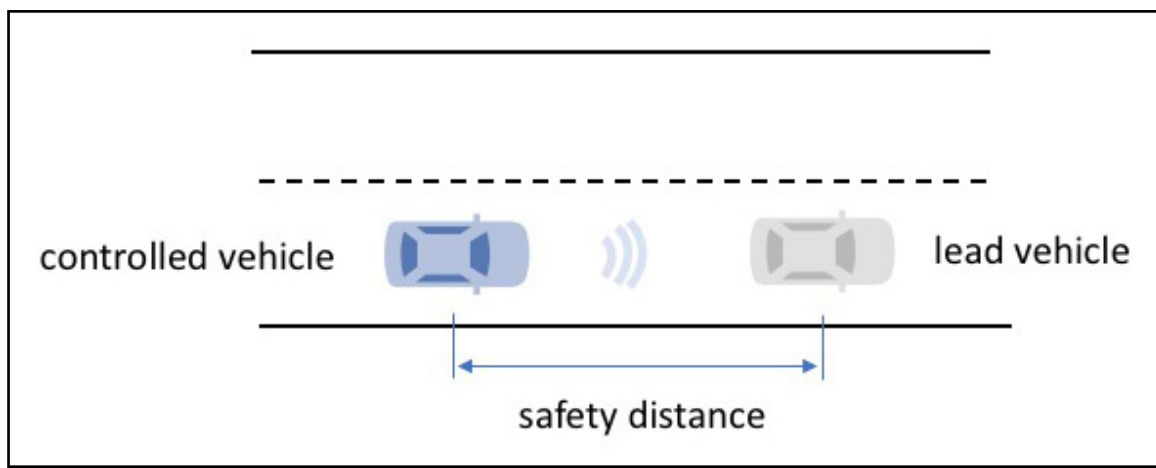


**Figure 2. Schematic Representation of Adaptive Cruise Control Function**

*Note: Lead Vehicle Determines Speed Control on Back Vehicle to Maintain Longitudinal Separation (i.e., a Given Safety Distance).*

Previous research in transportation-networks simulation has focused on the notion of multi-agents, where each of multiple agents (i.e., each vehicle) is modeled as a separate entity, but the same laws apply to all agents for controlling their motion within the simulation (Cetin et al., 2002; Burmeister, Haddadi, and Matylis, 1997). Particle swarm is another instantiation of how a multi-agent framework can work, and allows generalization of the concept represented in Figure 2 to that of Figure 3, where “multi-body leads” are used to define and control the movement of the controlled AV. In this case, an entire family of vehicles (i.e., the swarm) within a prespecified neighborhood is used as reference for the motion of the controlled vehicle.

In the situation depicted in Figure 3, the controlled vehicle uses all the surrounding vehicles that are part of the swarm to maintain both lateral (across lanes) and longitudinal (within lane) separation. It thus achieves an improved control over the typical ACC application, which can only control longitudinal separation (i.e., forward/backward direction). The application of particle swarm motion would also allow optimizing traffic as the AV senses relative position and speed of both forward lead vehicles as well as of those in the back through this approach.

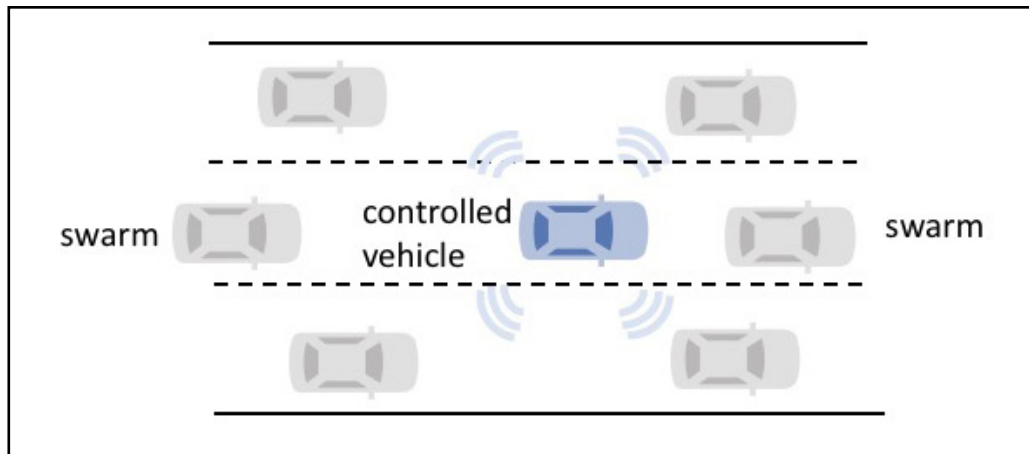


**Figure 3. Schematic Representation of a “Multi-Body” Swarm-Type Control**

The work presented in this report addresses how the rules of particle swarm motion can be adapted to monitor vehicles’ operations and achieve a scenario such as that of Figure 3. This adaptation will leverage the notion of hazard level or danger index, a concept typically used in robotics that measures the “closeness” of a system to a given accident scenario (Favarò and Saleh, 2016). Several quantifiable metrics will be devised in the form of hazard levels for swarms of AVs to monitor the concurrent motion of the swarm and trigger changes in the vehicles’ lateral and longitudinal movement while ensuring separation. Although there are no constraints on this work’s implementation, it is expected that it would be most relevant for highly automated Level 4 and Level 5 vehicles, capable of communicating with each other, and in the presence of a monitoring ground control center for the operations of the swarm. The argumentation that follows is general in nature, and the level of automation of the car does not restrict the applicability of the hazard level indices developed in this work. It is a prerequisite, however, that the vehicles in the swarm be capable of either estimating through proper sensors or of getting via direct communication (through vehicle to vehicle communication—V2V) each other’s speed and relative distance.

## II. AN OVERVIEW OF PARTICLE SWARM

### THE ORIGINAL USE: PARTICLE SWARM OPTIMIZATION AND RULES FOR MINIMUM FINDING

Particle Swarm Optimization (PSO), introduced by Kennedy and Eberhart (1995), is an iterative method for solving optimization problems involving nonlinear objective functions. In simple terms, this algorithm is used to find the unknown location of the minimum of a known function, as presented in Figure 4.

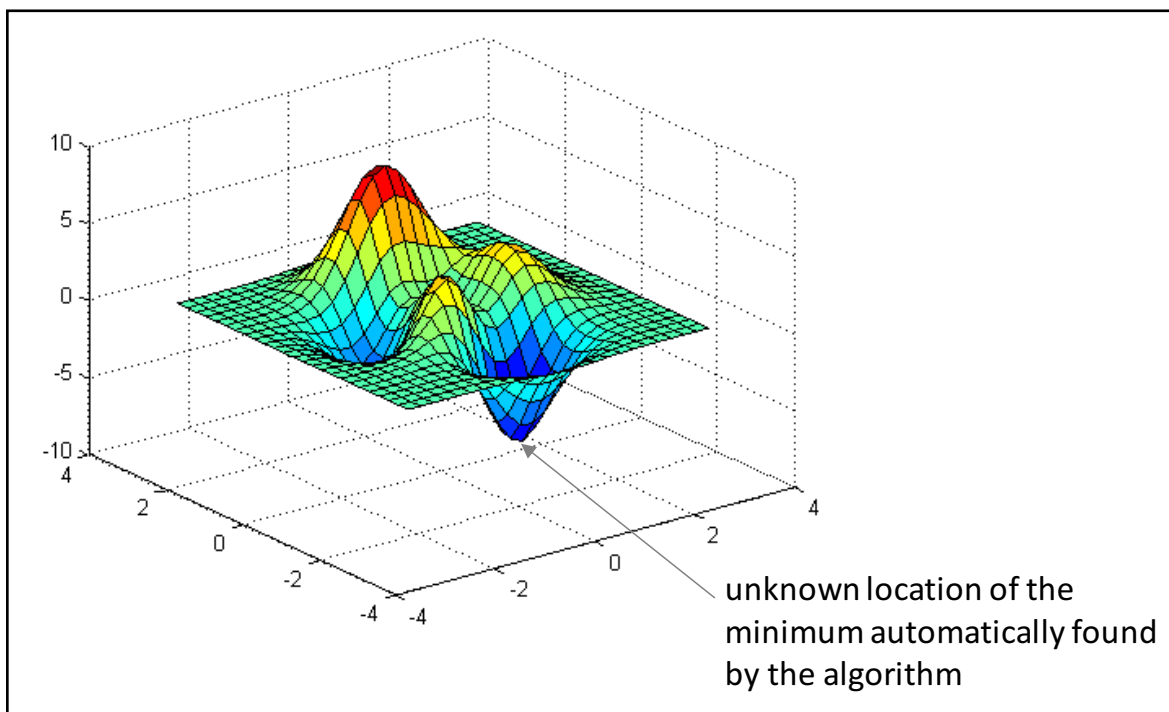


**Figure 4. Visual Representation of the Minimum-Finding Original PSO Algorithm for a Sample Nonlinear Function**

The PSO algorithm leverages an analogy with the synchronized movement observed in nature in fish shoals and bird flocks (Kennedy and Eberhart, 1995). The algorithm works by generating a family (or swarm) of particles that iteratively “sample” the known function and then update their position to resample the function in different locations. The position update (or swarm movement) is based on a combination of the information obtained from all the particles in the swarm (Shi and Eberhart, 1999). The movement of the swarm towards the correct solution is achieved by weighting more the information coming from those particles that turn out to be closer to the solution (and provide thus a lower value of the objective function) and moving the swarm in that direction. All the particles in the swarm move according to three fundamental laws based on nature observation, and originally formulated by Reynolds (1987):

1. maintaining separation: each particle moves to avoid collisions with other particles in the swarm;
2. maintaining alignment: each particle steers in the average direction which the swarm (or a neighboring subset of it) is pointing towards; and
3. maintaining cohesion: each particle moves towards the average location of the entire swarm without drifting too far off the center.

The three rules are schematically represented in Figure 5.

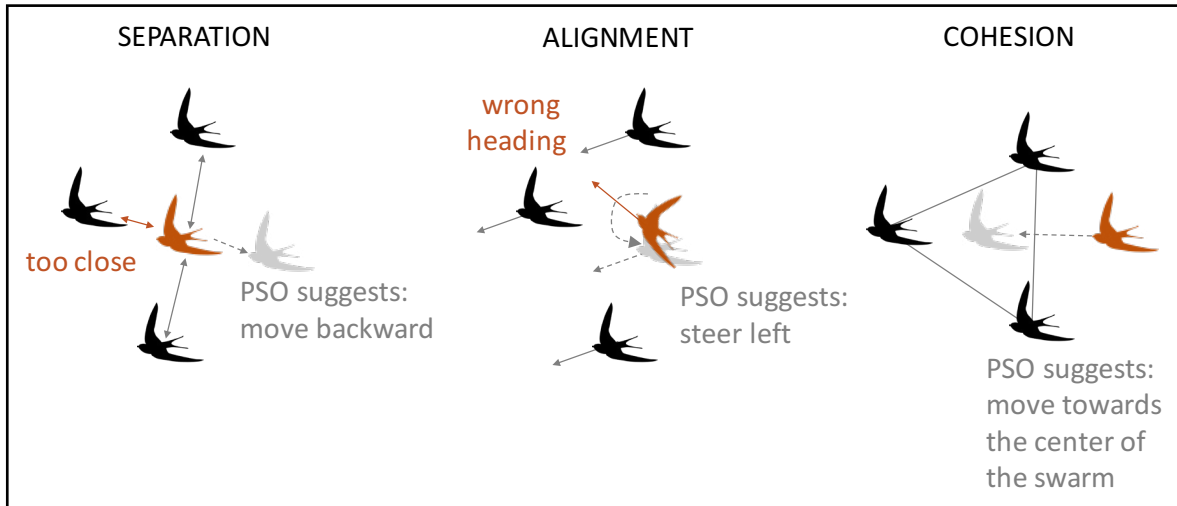


**Figure 5. The Three Swarm Rules Identified by Reynolds (1987) and Suggestion for the “Particle” Motion According to PSO**

In the algorithm developed by Kennedy and Eberhart (1995), each particle remembers/stores its position and the value of the objective function at that position. The particles are also aware of the global best for a particular iteration (i.e., the location of the particle that did the best job at getting close to the minimum at that iteration) through communication with the rest of the swarm. The algorithm works iteratively by subsequently changing all the particles’ positions until they converge to the optimum value for the specific objective function under investigation.

## ADAPTING PSO TO VEHICLES CONTROL

The original algorithm proposed by Kennedy and Eberhart can be generalized to n-dimensional problems, and is most commonly used for 3-D objective functions (such as the one shown in Figure 6). This commonality also comes from the natural observation of birds and fish swarms that indeed move within a three-dimensional space. In the realm of ground transportation two dimensions are used, so that in the following discussion we always refer to a 2-D world with a lateral motion (that controls side movement across lanes) and a longitudinal motion (that controls the forward/backward movement of the vehicle). This is visually represented in Figure 6.

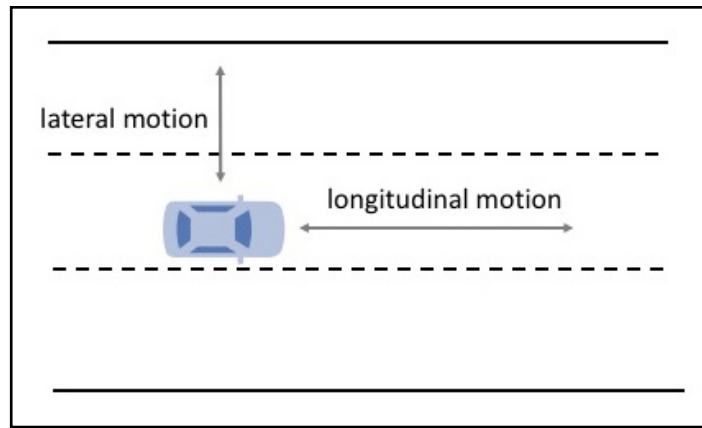


**Figure 6. Possible Principal Directions of Movement in a 2-D Context**

The generic position of a vehicle can thus be identified by three variables: two coordinates ( $x$ ,  $y$ ) to identify its location, and an angle to identify its heading within the two-dimensional space (Figure 7).

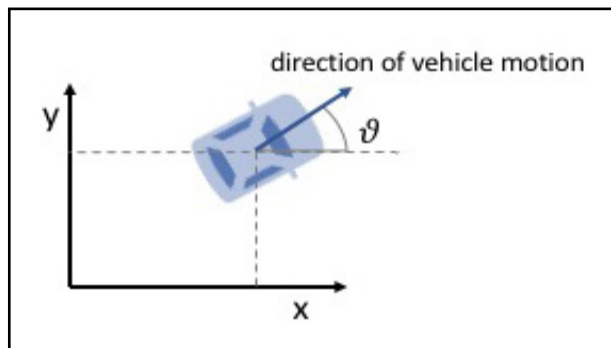


**Figure 7. Coordinates Used to Identify Vehicle Location and Heading**

In general terms, all the laws observed by Reynolds could be applied to families of vehicles. However, we need to consider that the end goal is that of providing steering and acceleration/breaking inputs to the algorithm that handles the vehicle control. For such a purpose, it becomes apparent that the “cohesion” law may not be suited in all scenarios (for instance, we would not want a vehicle to swerve left and right within its lane just to get in the center of the other vehicles), and that in a way all three laws (in their original formulation) can be subsumed under the generic principle of collision avoidance.

For this reason, we adapted the original three PSO laws to the following three rules for lateral and longitudinal motion control in autonomous vehicles.

1. Collision avoidance—maintaining separation to avoid collision with the nearby vehicles
2. Heading selection—maintaining the weighted average heading to neighboring vehicles
3. Velocity matching—matching the average velocity of the neighboring vehicles

Collision avoidance is based on the position of the vehicles rather than their instantaneous (i.e., current) velocities. Collisions are avoided by maintaining a certain amount of separation between the vehicles for both longitudinal and lateral separation, given that a vehicle continuously moves in a combination of both directions. Figure 8 shows the controlled vehicle moving away from the other vehicles to avoid a collision.

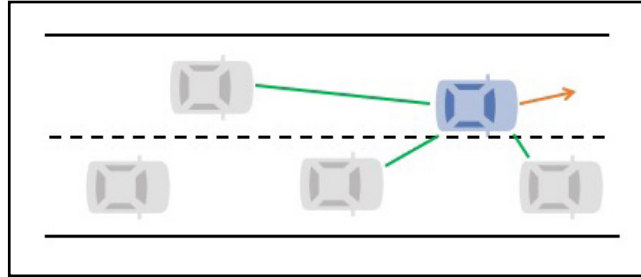


**Figure 8. Generic Representation of Collision Avoidance**

Heading selection is based on the heading of the neighboring vehicles within the “swarm.” For transportation purposes, rather than referring to an actual swarm, it is preferable to refer to neighborhoods of vehicles or vehicle cluster, which is the technical term employed going forward. If the rest of the cluster is changing its heading, then the controlled vehicle will also change its heading to match the average heading of the cluster. Heading selection ensures lateral and longitudinal control by modifying the direction of the vehicle velocity vector (through a steering input) so that the vehicle follows the average heading of the surrounding vehicles. This implies that a vehicle that has a malfunctioning camera or that is for some reason unable to detect lane markings will still be able to follow the proper traffic flow by steering in the average direction in which the surrounding vehicles are steering (provided at least one of them is capable of recognizing the road direction and V2V is enabled). Figure 9 shows a representation of this concept where the controlled vehicle adjusts its heading based on a weighted average of the surrounding vehicles headings (implementation details will follow in the next section.)

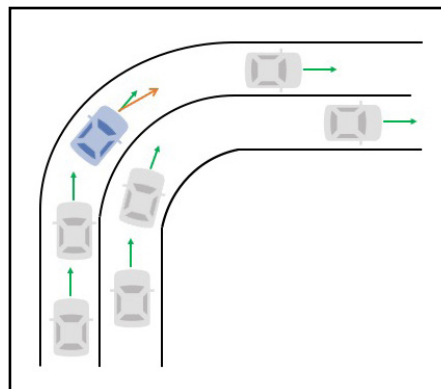


**Figure 9. Generic Representation of Weighted Heading Selection**

The final rule we set up for vehicles control is that of velocity matching. Indeed, separation and cohesion are two sides of the same coin, and in autonomous vehicles' motion both factors can be integrated within collision avoidance. We thus preferred to generalize a third law to control vehicles' speeds. This new law is based on the velocity of the neighboring vehicles instead of their positions. Notice that the velocity matching requirements takes care of cohesion in a strict sense (no vehicle gets left behind) as well as of traffic flow improvement. This is an important factor, because the traffic moving at the same speed can avoid phantom traffic jams (traffic congestions caused by small disturbances) (Kurtze and Hong, 1995) which can increase efficiency, and save fuel and time. In the original algorithm, this is done by assigning each vehicle the velocity of the nearest neighboring vehicle (Kennedy and Eberhart, 1995). This process can be adapted to ensure that the vehicle's speed matches the average of the closest vehicles within its neighborhood (Figure 10), similarly to what is proposed for vehicle heading.

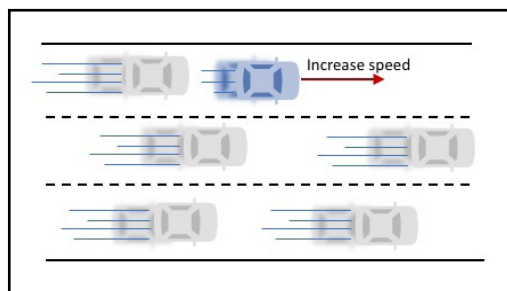


**Figure 10. Schematic Representation of the Velocity Matching Concept**

Although particle swarm motion is relatively new in the context of autonomous vehicles, there is a body of literature on multi-agent systems and the cohesive behavior of transportation networks. Swarm modeling has been studied and applied to a family of robots collaborating towards a specific task (Liu, Passino and Polycarpou, 2003; Suzuki and Yamashita, 1999). More recently, its application to autonomous vehicles has been investigated by Fredette and Özgüner (2017), who developed swarm-inspired modeling to describe the interactions of vehicles on a two-lane highway. Although we tackle the same application (albeit not restricted to two lanes as the hazard level definition is general), the approach employed and the scope of the work is substantially different. In a way, the approach of Fredette and Özgüner (2017) and ours are complementary in nature, with this work focusing on a system safety perspective and thus tackling the monitoring of danger indices to define safety regions of operations for each vehicle in the swarm. In Fredette and Özgüner (2017), vehicles in the swarms have different desired speed, and model different “driver types” (“grandma”, “jack”, and “teenager”). The authors focus on ensuring stability of the framework from a control-theory standpoint. The bulk of multi-agent research published to date is aimed at simulating and modeling the movement of conventional vehicle—see for instance (Cetin et al., 2002; Burmeister, Hadadi, and Matylis, 1997)—in contrast with the research proposed here. Similarly to (Fredette and Özgüner, 2017), we are here investigating high-level frameworks for cooperative control design.

Moreover, particle swarm optimization (in its original minimum-finding capability) has also been a focus of recent research related to autonomous vehicles. This use is fundamentally different than what is proposed here, as we are not making use of the optimization algorithm

per se. Worth mention in this category is the work by Hunaini, Robandi, and Sutantra (2016) who used PSO to optimize the parameters of a PID- (Proportional-Integral-Derivative)-controlled for automatic steering and also implemented a fuzzy logic controller.

---

### III. SWARM MOTION IMPLEMENTATION AND HAZARD-LEVEL MONITORING

#### THE NOTION OF DYNAMIC CLUSTER

Before looking at the actual implementation of the swarm monitoring, it is necessary to define which vehicles are part of the swarm and are thus going to be used as a reference. Given the preliminary nature of this investigation, the authors are going to consider a steady state of the swarm, with vehicles already present in the controlled environment. The problem of new vehicles entering the swarm is preliminarily addressed with the velocity-matching hazard level presented next, while the problem of vehicles exiting the swarm is left as a future avenue for this work.

Vehicle clusters contain a limited number of vehicles that are used as a reference to compute the control inputs for the vehicle under consideration. As a first approximation, a cluster (or family of vehicles) can be formed based on the distance between the vehicles, possibly setting a limit on the maximum number of vehicles we want to consider. More advanced rules for cluster definition can also be set up, for instance depending on the width of the road (number of lanes) or on current traffic density.

Equally important is understanding that a cluster is a dynamic concept that can continuously change in time. For instance, considering a highway environment, cars will continuously enter or exit the limited-access road, so that it is not desired to keep the same vehicles within the cluster at all times. It is thus possible to establish different “modes of operation.” A simple breakdown can be established as follows:

1. Steady-state mode: vehicles in this mode of operation already have an established cluster that is used as reference to determine steering and acceleration/deceleration control inputs. One can think of this mode as the “cruising” mode of the vehicle.
2. Transient mode: vehicles in this mode require a new cluster definition based on their need to enter or abandon the major flow of vehicles that they were previously following;
3. Emergency mode: vehicles in this mode are required to adapt their cluster to let other traffic with high priority (such as emergency vehicles) pass through;
4. Idle mode: vehicles in this mode do not require a cluster definition. This is the typical situation of parked vehicles that do not need to take into consideration what the surrounding traffic is doing.

More refined modes of operation for cluster definition can of course be defined, but at this preliminary investigation stage we will focus on the steady state and the transient mode.

Figure 11 shows a possible diagram for the formation of a new cluster based on two constraints: one on the maximum distance from the vehicle to control, and one based on a maximum number of vehicles. The process of Figure 11 first checks that a maximum

distance is not exceeded as well as that the vehicle is travelling in the same direction of motion (so it is not in an opposite direction lane). Afterwards, the same process checks that the cluster formed does not exceed the maximum allowed size. Should that be the case, a secondary check on the vehicle's distance is considered to sort vehicles within the cluster by distance and reject those that are further away.

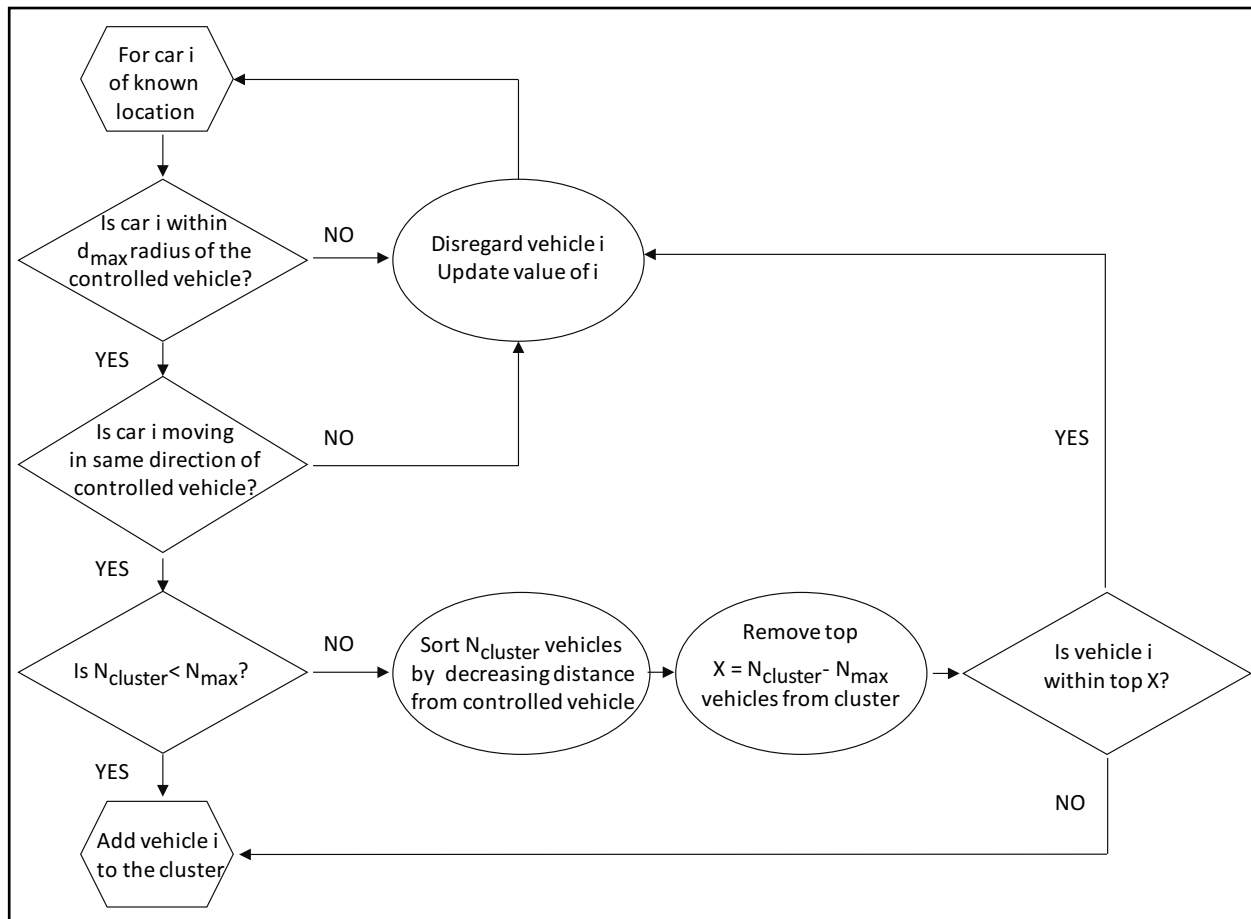


**Figure 11. Flow Diagram for Cluster Definition Based on Distance and Maximum Size**

To apply the process described in Figure 11, it is necessary to determine the radius of action of the cluster ( $d_{max}$ ) and the ideal size of the cluster (in terms of numbers of vehicles included). Also note that for the process to work, the vehicles need to either be able to communicate with each other (V2V communication) and share the respective location, or need to have functioning sensors (e.g., camera, Radar, or Lidar) to determine relative position. For the purpose of this preliminary work, the investigators found that a possible upper threshold for the radius of action should be close to 286 ft. This datum is computed by considering the average speed limit in limited-access roads (that is, 65 mph) and a conservative estimation of the time headway employed by currently deployed-on-the-market cruise control systems (ranging between 1.1 and three seconds (Malakorn and Park, 2010; Nowakoskwi et al., 2010)). The vehicle's time headway is defined as the time taken for a vehicle to travel the inter-vehicle spacing ahead of it (Li and Shrivastava, 2002). Taking the preceding into account, we can consider an acceptable radius to be:

$$d_{max} = 3 s \cdot 65 \frac{mi}{hr} \cdot \frac{1}{3600} \frac{hr}{s} \cdot 5280 \frac{ft}{mi} = 286 ft$$

The value of the radius can be adjusted in more refined approaches based on the traffic flow. In general terms, the radius allows definition of a first family of vehicles. Once this initial reference family based on distance is established, the process of Figure 11 starts applying more restrictive rules to narrow down the cluster size. First, it iterates through the vehicles within the radius of action and removes all those which are moving in the opposite direction. Second, it checks the size of the cluster. If we refer to  $N_{cluster}$  as the current number of vehicles within the cluster, we need to check that  $N_{cluster} < N_{max}$ , where  $N_{max}$  is the maximum number of vehicles within the cluster. In an ideal situation, we could keep  $N_{max}$  as low as 8, for a scenario in which every neighboring spot is occupied, such as shown in Figure 12.

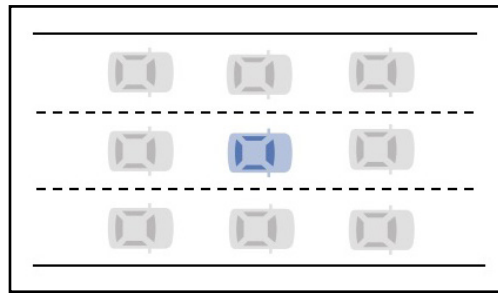


**Figure 12. Cluster with Eight Neighboring Spots Filled. Here the Radius of 286 ft. Gives a Swarm Width of 572 ft. (Three Vehicles in the Longitudinal Direction)**

When not all neighboring spots are occupied, the value of  $N_{max}$  can be increased, and a method that weights more the contribution of vehicles that are closer can be implemented as presented in the next section. Moreover, if  $N_{cluster} > N_{max}$ , then the process proceeds to rank all the vehicles based on their distance from the controlled vehicle. For instance, the vehicles indices can be arranged in decreasing order, with the top  $X = N_{car} - N_{max}$  vehicles then discarded from the cluster. Finally, for situations in which not enough vehicles are present, this framework reverts to the ACC model of a master-slave, with the controlled vehicle copying speed and heading of the vehicle in the front while maintaining a safety distance (so that the minimum number of vehicles in the swarm would be two, with the lead vehicle following instructions from a GPS-based system or a ground control center).

This section presented a preliminary investigation on cluster formation. Recently, authors have started to look into the problem of cluster formation, especially with a focus on enabling V2V communication in restricted ranges (i.e., only between vehicles within the cluster) (Özkul and Çapuni, 2014; Allouche and Segal, 2013). Once the cluster is formed, each vehicle within the cluster uses the information from the other ones to continuously update its own heading and speed (based on steering and acceleration/deceleration inputs) to satisfy the three rules of the particle swarm (i.e., avoid collisions, select best heading, and match velocity to optimize traffic flow). But how are the three rules actually implemented? In the following the researchers will introduce the notion of hazard level and see how such a concept can be used to trigger a change in speed and heading for the vehicles in order to ensure safety of operations.

## THE NOTION OF HAZARD LEVEL

The hazard level (also called danger index—with the two terms used interchangeably hereafter), is a concept originally invented in robotics and then adapted by Favaro and Saleh (2016, 2018) for analyzing safety constraints in complex engineering domains. Intuitively speaking, the hazard level, denoted by  $H(t)$ , can be conceived of as the closeness of an accident to being released (Saleh et al., 2014). Its definition provides an index to quantify “how dangerous” the current system state is, in terms of its proximity to an accident occurrence.

In general terms, we can model any accident sequence as a series of events. More specifically, in the case of an accident, a series of adverse events will bring a system from its nominal operational conditions to off-nominal ones and finally to an accident occurrence (Favaro and Saleh, 2016; Favaro and Saleh, 2018). This escalation can be reflected by the dynamics (or behavior in time) of the hazard level over time, as shown in Figure 13.

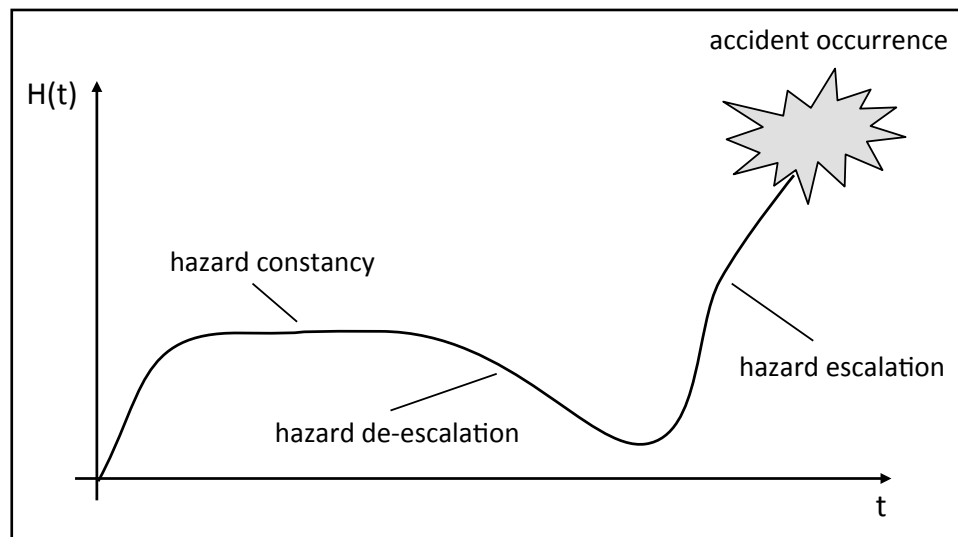


**Figure 13. Hazard Level Dynamical Behavior in Time**

*Note:* Favaro and Saleh, 2016, 2018.

The dynamics of the hazard level are not necessarily monotonic, and they can consist of a sequence of escalation, de-escalation, and constancy phases. Safety interventions are meant to block or de-escalate a hazardous situation (or its hazard level).

The notion of hazard level helps better define what adverse events to monitor against. By defining specific values of  $H(t)$  to stay clear from, one can monitor the system for how close it is to something one wants to avoid. Intuitively, the implementation of this requirement in a quantifiable form implies the verification of the following constraint for the hazard level:

$$H(t) < H_A$$

where  $H_A$  represents the hazard level associated with the onset of a specific accident/hazardous condition to avoid. For example, in the context of ground vehicles, simple hazard indices can be set up to monitor a threshold against speed limits. A simple constraint to ensure speeds are maintained within safe bounds could be set up as:

$$H(t) = \frac{v(t)}{v_{safe}}$$

This way the hazard level grows from a value of zero (when the vehicle is still) to a value of one or above when the speed limit defined by  $v_{safe}$  is reached. Different safety speeds could be defined for different roads/conditions (e.g.,  $v_{safe} = 65$  mph for ideal highway conditions, or 20 mph in school zones, or 35 mph near construction areas, etc.). The computation of  $v(t)$ —the vehicle speed—would come from integration of the differential equations that model the vehicle motion once acceleration/deceleration inputs are known, as well as external conditions that affect the speed of the vehicle (e.g., wet or icy roads). In this simple case, one would want to stay within the limit provided by the situation  $H(t) = 1$  which the investigators thus define as their  $H_A$ , implying:

$$\text{safety requirement: } H(t) < H_A \text{ with } H_A = 1 \rightarrow v(t) = v_{safe}$$

Note that all hazard level functions defined in this work are nondimensional. Properties such as the one expressed above allow the setup of safety bounds (or safety envelopes for higher dimensions than 1D) and criticality thresholds for the hazard level. Safety margins can also be accounted for in the definition of the threshold values, so that in general it is required that  $H(t) < H_{crit}$ , for a pre-defined  $H_{crit}$  criticality threshold. This concept can be translated into a plot of “criticality regions” as conceptually presented in Figure 14, with specific thresholds that can warn a driver of getting too close to the allowed limit. It can potentially provide a warning of situations in which a lower speed range should be kept (for instance, in case of possible hydroplaning on wet roads, the system can provide a warning at the recommended speed, also based on the specific tire inflation of the vehicle). Figure 14 shows the dynamics in time of the hazard level for speed control obtained for a sample acceleration profile of a small vehicle entering a highway environment from an initial speed of 30 mph. As the vehicle accelerates to merge with traffic (acceleration profile as provided in (Meher, Chandra, and Velmurugan, 2013) its speed gets closer to the  $v_{safe} = 65$  mph limit of standard highway operations. A critical threshold set up for  $H(t)_{crit} = 0.85$  (i.e.,  $v(t) = 0.85 * v_{safe} \sim 55$  mph) provides a trigger to reduce acceleration towards maintaining a constant value of speed (plotted in Figure 16 are the first 100 s of acceleration).

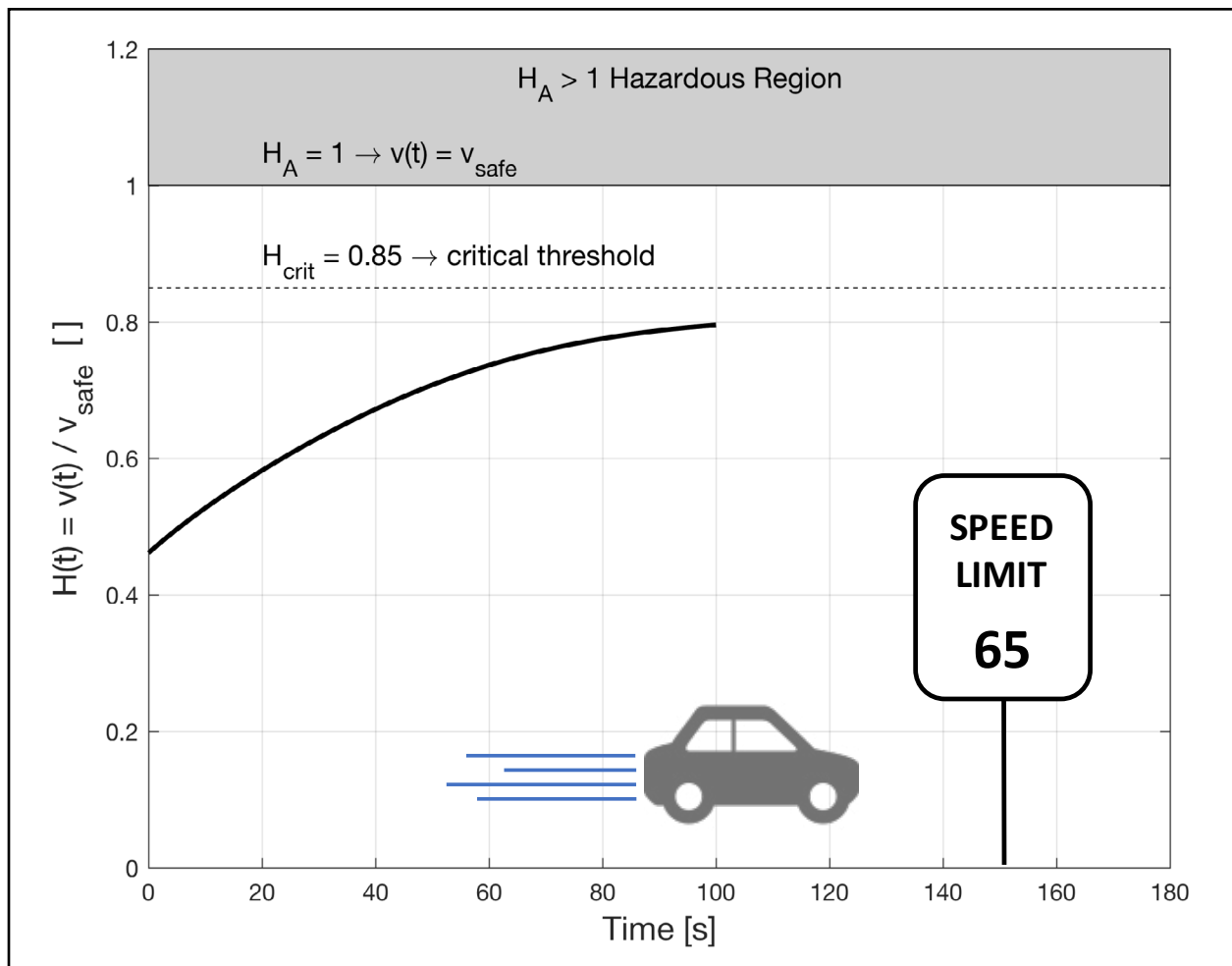


**Figure 14. Example Hazard Level Dynamics for  $H(T) = V(T)/V_{safe}$**

Note: The System Models a Vehicle Accelerating to Merge with Traffic on a Highway, from a Starting Speed of 30 MPH. Safety Speed Considered is 65 MPH. Acceleration Profile for Standard Vehicle Provided in (Mehtar, Chandra, And Velmurugan, 2013).

Plots such as the one of Figure 14 can serve as a diagnostic tool to inform safety interventions. For instance, in this case a value of  $H(t)$  too close to  $H_A$ , and a sustained positive slope for  $H(t)$ , suggests that a safety intervention is warranted—at a minimum to block the dynamics of hazard escalation through emergency braking for example, and slowing down to de-escalate the hazardousness of the situation and decrease the vehicle speed. Of course, this is a simplification for explanatory purposes only, as a vehicle traveling too slow or braking too suddenly would pose a hazard to other traffic. Actual implementations of the hazard level function for PSO motion are properly developed next.

## CREATING SAFETY TRESHOLDS FOR SEPARATION CONTROL BASED ON THE THREE PARTICLE SWARM RULES

Within the Particle Swarm Optimization algorithm, particles move during their search for the objective function optimum by iteratively updating their position and their velocity vector according to the following two rules:

$$v_{i+1} = v_i + \text{correction by PSO}$$

$$d_{i+1} = d_i + \text{correction by PSO}$$

The correction is computed by considering a combination of what PSO calls the “local best” and the “global best.” In this approach, each particle communicates with the others, and the swarm can globally determine which particles have a better shot of finding the function minimum based on the historically best performance of each particle.

In this application, this line of thought is not suitable (as one does not want the vehicles to converge to a given point—that would simply cause a major collision), and the iterative update of velocity and distance needs to be based on the three rules we previously decided to adopt, i.e., collision avoidance, heading selection, and velocity matching. In practical terms, the researchers are going to use the notion of hazard level and the creation of safety thresholds for such quantity to trigger a change in the control inputs of steering and acceleration/deceleration. Such control inputs will drive the dynamic of the autonomous vehicle, and (once mathematically integrated within the system of differential equations that model the vehicle) will lead to the correction for updating velocity and position vectors of the autonomous vehicle.

In the following, the investigators are going to set up different hazard level functions that map each of the particle swarm adapted rules. The equation development is preliminary in nature, given the exploratory nature of this research. The goal of the present seed grant is in fact that of investigating feasibility of the proposed approach only.

## **Collision Avoidance**

Separation and cohesion of the original PSO algorithm were combined in our rule of collision avoidance. Such requirement translates into a careful monitoring of the distance (both lateral and longitudinal) between the vehicles that are part of the cluster.

We are going to start with a simplified look into the separation issue, leaving cohesion for next. At a minimum, separation should guarantee that in case of emergency braking, the vehicles have enough spacing to safely come to a stop without colliding with each other. It is thus possible to explore hazard levels and safety metrics related to the stopping distance of the vehicle. In first approximation, the vehicle movement along limited-access roads is mostly within the longitudinal direction. Indeed, for long periods of time, the vehicle heading coincides with the lane centerline and is not changing in the lateral direction. In those situations, a hazard level similar to the one presented in (Favarò and Saleh, 2016) for aviation applications can be adapted to the case of ground vehicles.

Consider thus two vehicles travelling longitudinally, as presented in Figure 15. Each vehicle is characterized by a position changing in time as well as a speed (which we consider in the longitudinal direction only for now). In Figure 15 we note the relative distance between the two vehicles as  $d(t)$ .

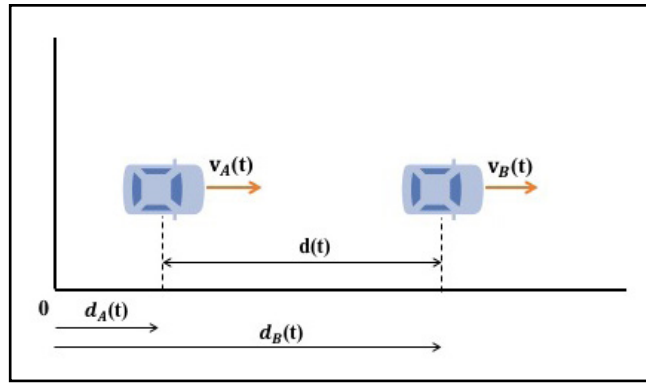


**Figure 15. Representation and Notation used for the Case of Two Vehicles (A and B) Travelling Longitudinally**

With the goal of ensuring that each vehicle is allowed to stop without colliding with one in front of it, it is possible to set up the following hazard level:

$$H(t) = \frac{d_{stopA}(t)}{d_B(t) - d_A(t)} = \frac{d_{stopA}(t)}{d(t)}$$

The equation relates the stopping distance for the vehicle behind  $d_{stopA}(t)$  to the relative distance between the two vehicles  $d(t)$ . The situation  $H(t) > 1$  identifies a collision, as it is indicative of a stopping distance required greater than the relative distance between the two vehicles. The accident threshold is thus defined as  $H_A = 1$ . The stopping distance depends on a number of factors, including environmental conditions (e.g., icy/wet road) and, of course, the initial speed at which the braking is initiated.

As first example, we can consider a simple model for the vehicle, assuming a constant deceleration and neglecting air resistance, road gradients and braking efficiency (more complex models can be easily developed and are beyond the exploratory scope of this work). In those situations, the stopping distance becomes a function of the initial speed of the vehicle and the friction coefficient between the tires and the road only, and is given by the equation  $d_{stop} = v_0^2 / 2\mu g$ , where  $v_0$  is the initial speed of the vehicle,  $\mu$  is the friction coefficient, and  $g$  is the gravity acceleration. In general, for a simple rigid-body one-degree-of-freedom system with constant deceleration, the following equations hold for each vehicle "i":

$$d_i(t) = \frac{1}{2} at^2 + v_{0i}t + d_{0i} \text{ where } t = \frac{v_i(t) - v_{0i}}{a} \text{ and } a = -\mu g \rightarrow d_i(t) = d_{0i} + \frac{v_{0i}^2 - v_i(t)^2}{2\mu g}$$

In general, the hazard-level function defined above for two vehicles A and B thus becomes:

$$H(t) = \frac{v_{0A}^2 / 2\mu g}{d_0 + \frac{v_{0B}^2 + v_{0A}^2 - v_B^2(t) - v_A^2(t)}{2\mu g}}$$

The above expression can be evaluated at different instants of time and features the initial relative distance between the two vehicles  $d_0$  as parameter ( $d_0 = d_{02} - d_{01}$ ), along with the speeds of the two vehicles and the road friction coefficient.

Figures 16 and 17 show the above-mentioned hazard level computed for a simple simulation in which the front vehicle is still (for instance at a red traffic light or in queue in a traffic jam) and the second vehicle is approaching from behind. The two figures plot contour levels of the hazard function for different values of initial speed and relative distance between the two vehicles when the braking maneuver is initiated. The plots highlight the contour  $H_A = 1$  that divides regions of relative distance/speed combinations that are safe in preventing a collision from those characterized by hazard levels greater than one. Moreover, the two plots are obtained for two different values of the friction coefficient: dry road in Figure 16 vs. icy road in Figure 17. As can be expected, hazard levels are higher in the situation of icy roads, and a smaller region of “safety” is accounted for in this situation.

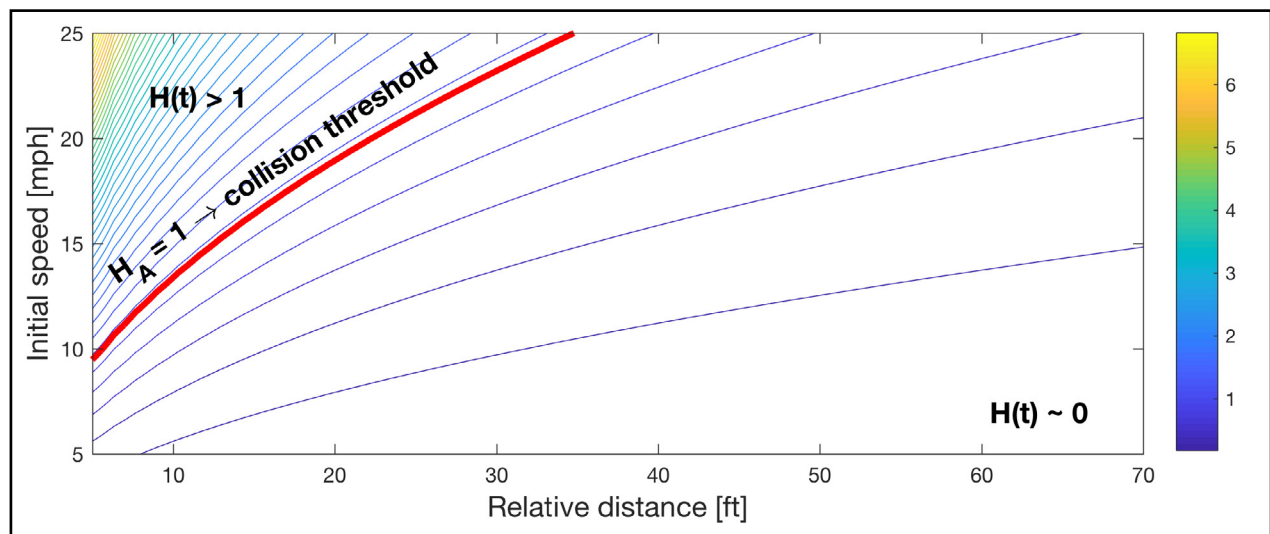


**Figure 16. Contour Levels for  $H(T)$  as a Function of Initial Speed and Relative Distance (Dry Road)**

*Note:* Ample Safety Region for Initiating a Braking Maneuver without Colliding with a Front Still Vehicle.

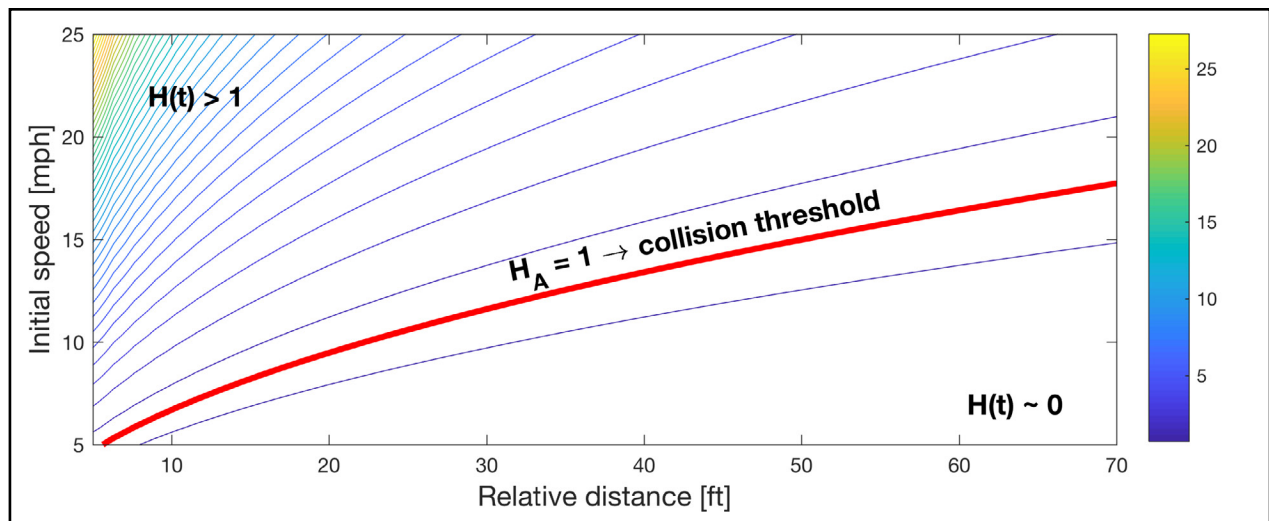


**Figure 17. Contour Levels for  $H(T)$  as a Function of Initial Speed and Relative Distance (Icy Road)**

*Note:* small safety region for initiating a braking maneuver even at low speed without colliding with a front still vehicle.

But how is this information used? At each point in time, a vehicle in the swarm is traveling at a given speed. Given that speed and the relative distance from the vehicle in front of it, it is possible to compute the hazard level  $H(t)$ . Values too close to one suggest that readjustments of speed or heading are needed to ensure separation. Values too close to zero suggest that readjustments of speed or heading are needed to ensure cohesion. This information thus serves as a diagnostic tool to trigger changes according to the other two laws of particle swarm. Additionally, this information needs to be checked for each vehicle within the swarm.

Figure 18 shows contour levels for the same hazard level computed in a different type of situation. In this case both vehicles are moving, and the hazard level is plotted as a function of the initial speeds of the two vehicles assuming an initial relative distance of 45 ft. and dry roads. Once more, we want to ensure that the vehicle remains within the safety region of  $H(t) < 1$  and that such a safety region is big enough to account for errors/oscillations in the actual performance of the two vehicles. Should the region be too small, the algorithm suggests to increase the relative distance by changing speed or heading according to the other two laws, and once more, the hazard level monitoring serves as a control trigger.

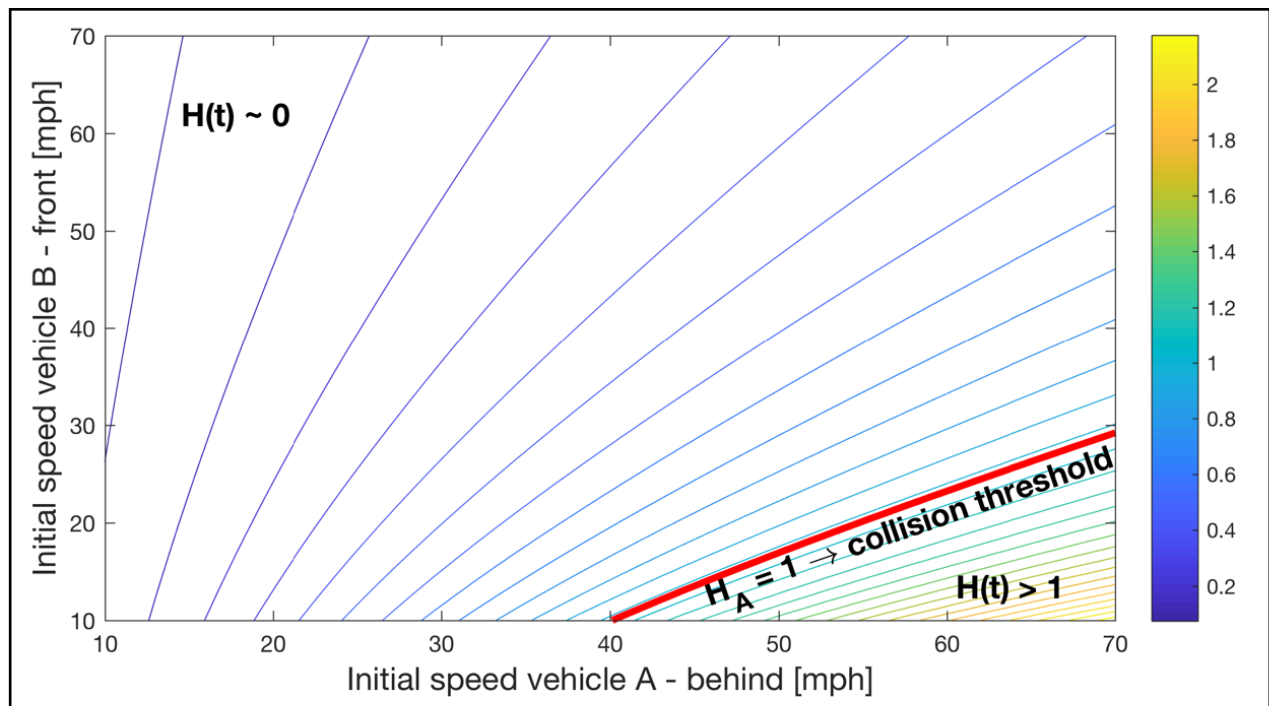


**Figure 18. Contour Levels for  $H(T)$  Based on Stopping Distance of Vehicle in Back When Both Vehicles Moving**

*Note:* Contours shown as function of initial speeds for both vehicles. Danger zones are entered when vehicle behind travels too fast compared to vehicle in the front.

The previous plots were obtained to account for a 1-D situation in which the vehicles are predominantly moving along the longitudinal direction. Hazard levels can also be computed for 2-D situations by generalizing the above discussion, and can account for cohesion assurance as well (i.e., ensuring that the vehicles are not too spread).

For the 2-D situation, it is possible to determine a “safety radius  $\varepsilon$ ” for each vehicle, and define thresholds to ensure that safety radii from different vehicles within the cluster are not intersecting. This concept is schematically represented in Figure 19 and is borrowed from the context of robotics, where it is sometimes referred to as the spheres of influence problem.

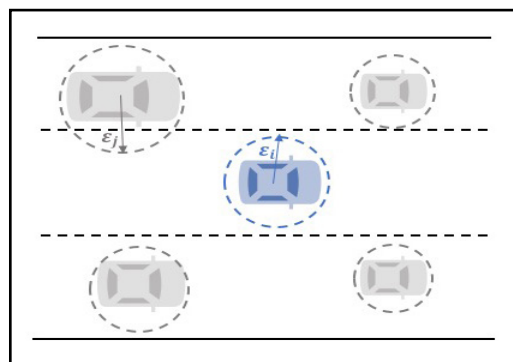


**Figure 19. Conceptual Representation of the Safety Radii for Vehicles of Different Dimensions**

In this case we need to consider that each vehicle position is a vector composed of both x and y coordinates. To ensure separation, it is possible to set up a hazard level that for each couple (i, j) of vehicles checks that their relative distance (vectorial) is greater than the sum of their corresponding safety radii. In other words, for each vehicle “i,” we check that there is no intersection within the sphere of any other vehicle “j” within the cluster. The corresponding hazard level is given by:

$$H_{i,j}(t) = \frac{\varepsilon_i + \varepsilon_j}{\|\vec{d}_i - \vec{d}_j\|} \text{ with } \vec{d} = \begin{bmatrix} x \\ y \end{bmatrix} \rightarrow H_{i,j}(t) = \frac{\varepsilon_i + \varepsilon_j}{\sqrt{(x_i - x_j)^2 + (y_i - y_j)^2}}$$

where d is a function of time and represents the position coordinates of each vehicle. This hazard level function reaches a value of one when the two safety radii touch (thus the vectorial distance is equal to the sum of the two vehicles’ radii). Once more, such a hazard level would need to be checked for every pair of vehicles present in the swarm. Values too close to one would prompt a change in speed and heading of both vehicles. Figure 20 shows an example of contours for H(t) for two vehicles with safety radii of eight ft. and six ft. respectively. The contour levels are in this case represented as a function of the relative position in both lateral and longitudinal coordinates, effectively representing regions of space in which the vehicle under control can move (all those with  $H(t) < 1$ ).

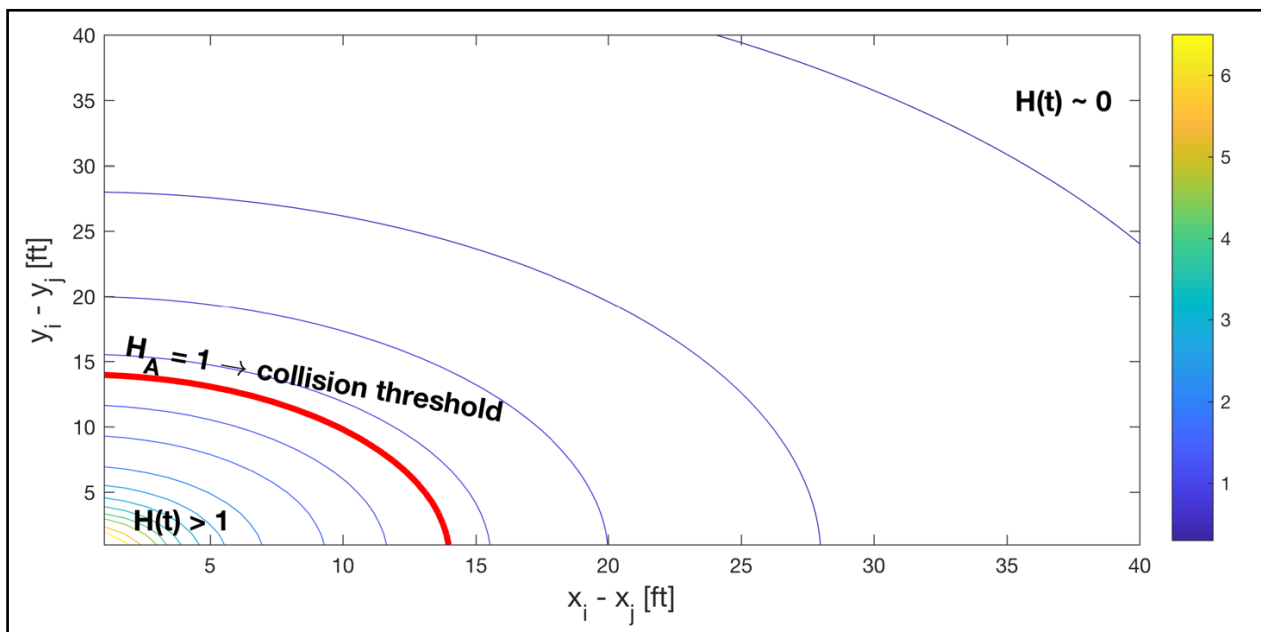


**Figure 20. Contour Levels for the 2-D Hazard Level Based on Spheres of Influence**

*Note:* safety radii considered: six ft. for vehicle I and eight ft. for vehicle J.

Note that this analysis is only preliminary, as at each instant of time we need to check vehicle “i” against all other vehicles in the swarm. This implies that whenever a position too close to  $H_A = 1$  is found, the vehicle cannot liberally be moved away from it. Before such movement is allowed, all the hazard levels against the other vehicles would need to be rechecked, leading to an optimization problem to minimize the overall combinations of (i, j) hazard levels. Moreover, the notion of a “box” of influence might be better suited for

traditional vehicles than a simple sphere. Additional areas for extensions, refinements, and future work are highlighted in the conclusions of this report.

Based on the previous analysis, it is intuitive that the problem of cohesion gets solved by imposing lower limits on the observed hazard level functions, thus avoiding values too close to zero. As mentioned before, cohesion is not of much relevance for Autonomous Vehicle (AV) applications, and separation has been the focus of this research.

The hazard levels investigated in this section (which model hazard monitoring against collisions) serve as triggers to changes in heading and speed. In other words, the rule of collision avoidance does not directly control the vehicle movement in our implementation. It rather serves as the initiating event by which changes in the control input (braking/acceleration and steering) are then executed. Such changes are investigated next with the remaining two rules for vehicle swarms.

## Heading Selection

The particle swarm rules dictate the existence of an average heading towards which each particle is moving. In the context of AV movement, we can adapt this notion to explore the possibility of computing each vehicle's heading as a weighted average of the headings of the surrounding vehicles. Figure 21 shows a representation of this concept when a middle vehicle (vehicle C) recalculates its heading based on the heading information communicated by two vehicles: one in the back (vehicle A) and one in the front (vehicle B).

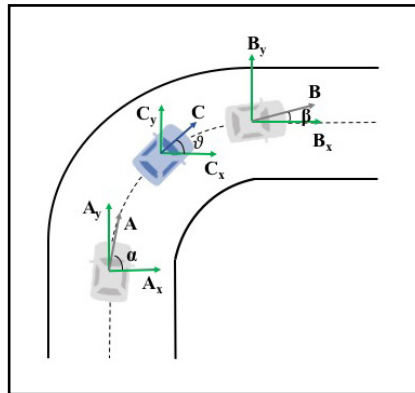


**Figure 21. Example of Heading Selection for a Middle Vehicle Based on Two Surrounding Vehicles' Information**

Depending on the actual configuration of the cluster, the rules for determining the vehicle heading will take into account different geometric configurations. In the example of Figure 21, we can compute the steering angle for vehicle C based on a modified version of the average headings of the cluster weighted through the distance from the vehicle we would like to control. We can thus define two quantities ( $d_1$  and  $d_2$ ) that represent the distances between the three vehicles:

$$d_1 = \text{distance between A and C}$$

$$d_2 = \text{distance between B and C}$$

We can then note that vehicle C is closer to vehicle B than to vehicle A, so that we would like to assign more weight to the heading of vehicle B. In other words, since vehicle B is closer, we expect the unknown heading of vehicle C to be closer to that of vehicle B than to that of vehicle A. The expected heading (and its steering angle) for vehicle C can thus be computed by taking a weighted average of the headings of both vehicle A and B, with B carrying more weight based on the distance between the vehicles. We can define:

$$A_x = \text{x-direction unit component of A} = \cos \alpha$$

$$A_y = \text{y-direction unit component of A} = \sin \alpha$$

$$B_x = \text{x-direction unit component of B} = \cos \beta$$

$$B_y = \text{y-direction unit component of B} = \sin \beta$$

By defining weights based on inverse distances (as we want the answer to be closer to the value of vehicle B which has a smaller distance) (Burrough, McDonnell, and Lloyd, 2015):

$$w_1 = \frac{\frac{1}{d_1}}{\frac{1}{d_1} + \frac{1}{d_2}} = \frac{d_2}{d_1 + d_2}; \text{ and } w_2 = \frac{\frac{1}{d_2}}{\frac{1}{d_1} + \frac{1}{d_2}} = \frac{d_1}{d_1 + d_2}$$

We obtain:

$C_x$  = x-direction unit component of C

$$C_x = \frac{A_x w_1 + B_x w_2}{w_1 + w_2} = \frac{A_x(d_2) + B_x(d_1)}{d_1 + d_2} = \frac{\cos \alpha(d_2) + \cos \beta(d_1)}{d_1 + d_2}$$

$C_y$  = y-direction unit component of C

$$C_y = \frac{A_y w_1 + B_y w_2}{w_1 + w_2} = \frac{A_y(d_2) + B_y(d_1)}{d_1 + d_2} = \frac{\sin \alpha(d_2) + \sin \beta(d_1)}{d_1 + d_2}$$

Thus, the unknown heading for the vehicle under control can be computed as:

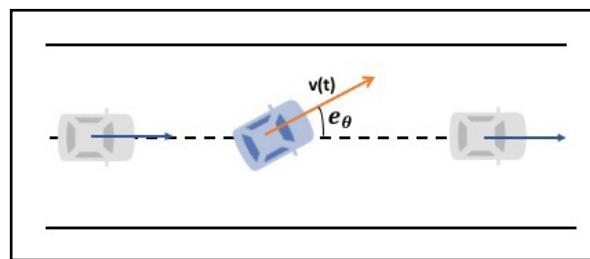
$$\tan \vartheta = \frac{C_y}{C_x} = \frac{\sin \alpha(d_2) + \sin \beta(d_1)}{\cos \alpha(d_2) + \cos \beta(d_1)}$$

$$\vartheta = \tan^{-1} \left( \frac{\sin \alpha(d_2) + \sin \beta(d_1)}{\cos \alpha(d_2) + \cos \beta(d_1)} \right)$$

The Inverse Distance Weights (IDW) method used above can be generalized for n vehicles in the clusters and can also be applied to the speed law of our adapted particle swarm motion.

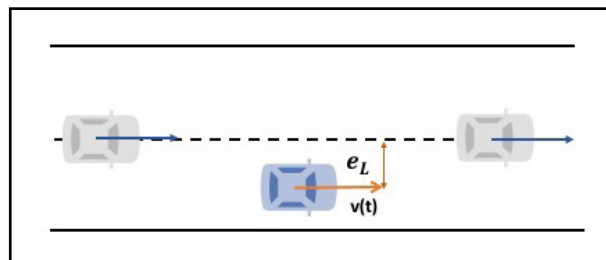
In general terms, for each “i-th” vehicle in the cluster, we will check a family of hazard-level functions for collision avoidance as presented in the previous section. Should those indicate values too close to one, a reassessment of the i-th vehicle’s heading and speed will be executed. In first approximation, headings can be computed with the method of IDW just presented, and once speed is also adjusted, the hazard levels can be periodically reevaluated to ensure all the vehicles remain in a safety region. This iterative process, especially for heading selection, needs also to be aimed at minimizing two position errors for each vehicle: an angular error and a lateral error. The two error checks can be implemented through a hazard-level function as presented next.

Figure 22 shows a visual representation of the notion of angular error. The angular error, denoted here by  $e_\theta$ , is defined as the angle between the vehicle heading and a given reference line (usually the center line of the lane).



**Figure 22. Angular Error Definition**

Similarly, Figure 23 represent the definition of the lateral error, here denoted as  $e_L$ . The lateral error is defined as the distance between the vehicle lateral position and the reference line, so that it indicates an offset of the vehicle from the reference line (so it is not a resultant of a previous angular error, as the angular error might be zero and the offset might still be present).



**Figure 23. Lateral Error Definition**

Assuming that the actual vehicle dynamics do not exactly follow the intended estimated dynamics predicted by the IDW (there will always be a minimal error in the estimation process and in the execution), error accumulation in time can lead to the general situation of Figure 24, where both a lateral and an angular error in the vehicle position are present.

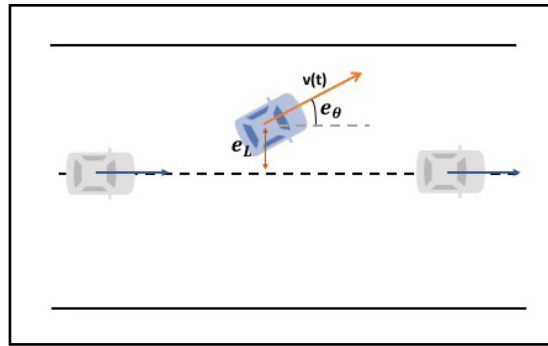


**Figure 24. Generic Situation Which Combines both Lateral and Angular Error**

The situation of Figure 24 becomes direr the closer one gets to other lanes and/or road dividers. Geometric considerations in the lateral direction lead us to define the following safety requirement:

$$e_L + v(t)t \sin e_\theta < \frac{w}{2}$$

where  $e_L$  is the distance in the lateral direction (the y axis) the vehicle travels in time  $t$ , and  $w$  is the total lane width. It is thus possible to set up the following hazard level:

$$H(t) = \frac{e_L + v(t)t \sin e_\theta}{\frac{w}{2}} = 2 \frac{e_L + v(t)t \sin(\theta_{actual} - \theta_{IDW})}{w}$$

where once more  $H(t) < 1$  is desired. Figure 25 shows an example evaluation of the hazard level above as a function of lateral and angular error for the situation depicted in Figure 24, where the front and the back vehicle are traveling straight along the reference line, and thus the predicted heading by IDW is 0 degrees. The parameters used in the simulation for Figure 25 are a lane width of 12 ft. and a target speed of 60 mph. (Many US highways have variable lane width in the range of 10-12 ft. The smaller the lane width, the lower the time interval  $t_{crit}$ .) As expected, the bigger the error the higher the hazard level. But what is the use of such a plot/hazard-level evaluation? As noted before,  $H(t)$  depends on the time at which it is evaluated. The more time the situation is left unchanged, the higher the hazard-level time (in Figure 25 we use a sample time of 1.5 seconds). This means that the hazard-level equation above can actually be used to find the maximum time before which the function reaches the critical level  $H(t_{crit}) = 1$  for a given error pair. This tells our algorithm that the vehicle heading and speed have to be refreshed at intervals lower than  $t_{crit}$ .

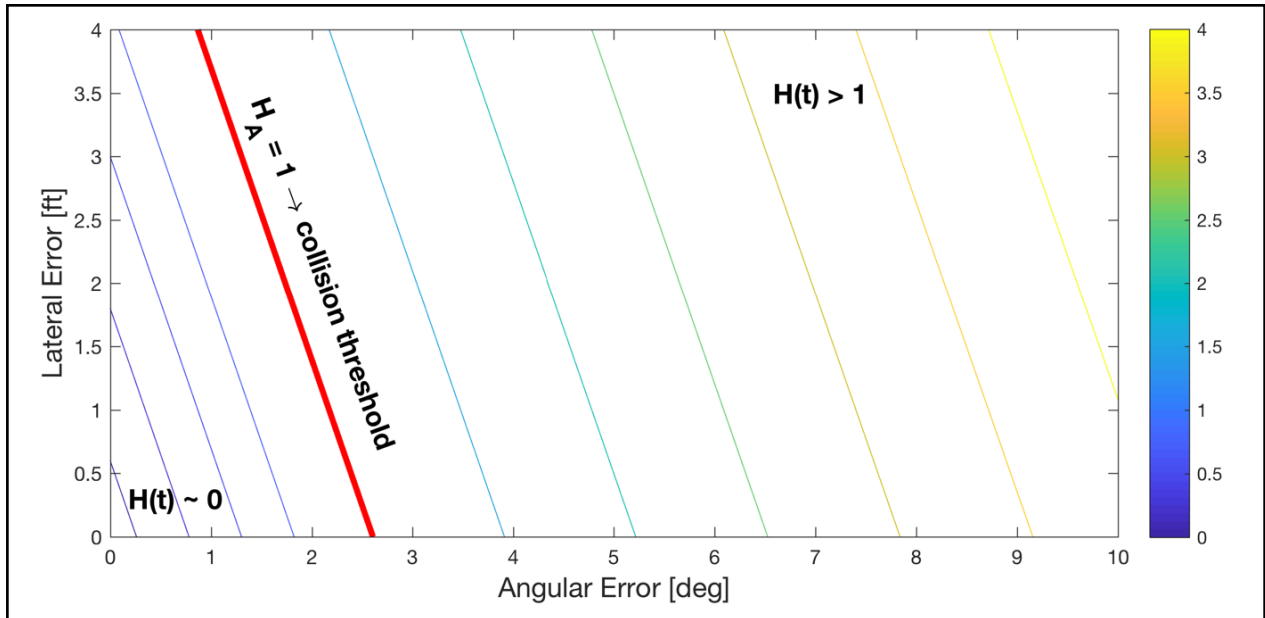


**Figure 25. Contour Levels for the Angular and Lateral Error Hazard Function**

Note: Sample situation with vehicle traveling at target speed of 60 mph, with offset position computed at 1.5 seconds. Standard lane width of 12 ft.

## Velocity Matching

The final rule adapted from particle swarm is that of velocity matching. Based on the previous discussion on IDW for heading computation, it is intuitive that the same approach can be used to compute a weighted average of speed based on the relative distance between the vehicles at each instant in time. Moreover, it should be clear (given the geometry of the problem), that if the IDW approach is computed for the two speed components along the longitudinal and lateral axis, the solution of the problem also gives the vehicle overall heading (assuming no vehicle slip for our simple rigid-body problem, thus guaranteeing that the velocity vector and the vehicle heading are aligned). The IDW equations for the two speed components are given by:

$$u_c = \frac{u_A d_2 + u_B d_1}{d_1 + d_2} \quad \text{and} \quad v_c = \frac{v_A d_2 + v_B d_1}{d_1 + d_2}$$

where the same notation of Figure 21 has been adopted, and where the velocity vector  $v(t)$  has been decomposed in the two components  $(u, v)$  along the two axes.

In simple situations where the swarm is already formed, the algorithm assumes that all the vehicles will be traveling at the same average speed  $v_{avg}$ . It is then possible to use the concept of velocity matching to better define the geometry of the swarm in terms of relative distance between the vehicles, target average velocity, and safety margins employed. This is done through the creation of one more hazard-level function set up in the following way. Imagine a new vehicle wants to enter the swarm (for instance, assume a vehicle enters the highway environment and wants to merge with the ongoing traffic as schematically represented in Figure 26).

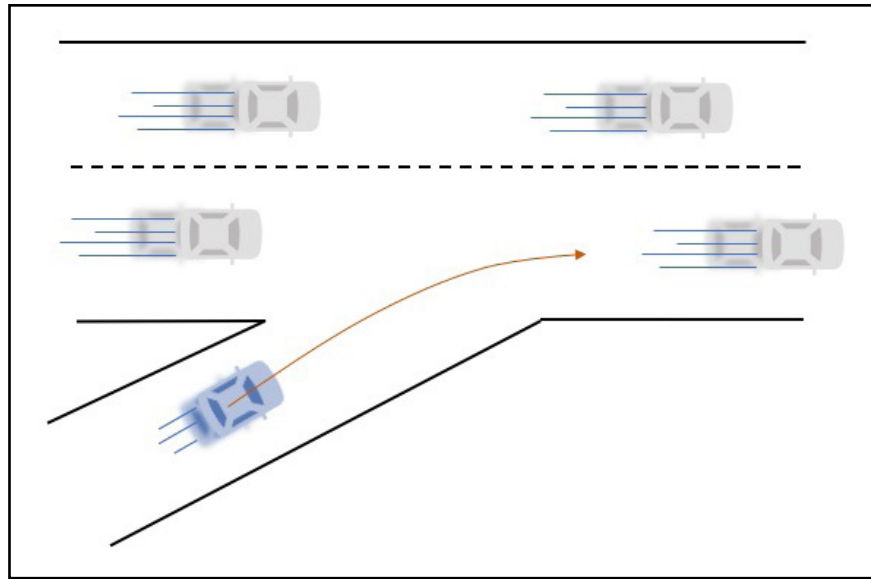


**Figure 26. Schematic Representation of a Vehicle Entering a Swarm**

The problem is that of adjusting the speed at which the swarm is travelling to accommodate the new vehicle, and of selecting the best distance between the vehicles that guarantees a smooth transition for the new vehicle. We define the following variables:

$t_{acceleration}$ : the time it takes the new vehicle to accelerate from its initial speed  $v_0$  to the average speed at which the swarm is moving;

$t_{passby}$ : the average interval of time that elapses between the instants at which two consecutive vehicles in the swarm pass by the same point. In other words, a vehicle belonging to the swarm will be occupying position  $x$  every  $t_{passby}$  seconds.

$SM_{time}$ : a safety margin expressed in seconds to ensure each vehicle that wants to enter the swarm has a margin when we compare the time required for it to accelerate and the time vehicles in the swarm are passing by.

We want to ensure that the following relation is satisfied:

$$t_{acceleration} + SM_{time} < t_{passby}$$

It is thus possible to set up the following hazard-level function:

$$H(t) = \frac{SM_{time} + t_{acceleration}}{t_{passby}}$$

where values below one of  $H(t)$  ensure there is enough time (with safety margin) for the vehicle to accelerate and merge with the traffic before another vehicle passes by. The acceleration time can be computed once the acceleration profile for the vehicle is known. Similarly to what is done for Figure 16, in the following we adopt a linear model for acceleration decreasing with speed provided by (Mehtar, Chandra, and Velmurugan, 2013)

for a standard sample vehicle. Integration of the acceleration vs. speed curve provides the time required to accelerate from a given initial speed  $v_0$  to the average speed at which the swarm is moving  $v_{avg}$ . The time of pass-by instead depends on the relative distance between the vehicles in the swarm and the average velocity  $v_{avg}$  (simply  $t_{passby} = \frac{d_{swarm}}{v_{avg}}$ ).

It is thus possible to plot the above hazard level as a function of the variables we wish to control. For example, Figure 27 shows the plot of the hazard level defined above as a function of the initial speed of the vehicle entering the swarm and the relative distance of the vehicles in the swarm. In the example of Figure 27, we are trying to target an average speed of the swarm of 65 mph, and we are employing a one-second safety margin. Intuitively, the closer the initial speed is to the value of the average speed, the closer the relative distance of the vehicles in the swarm can be kept.

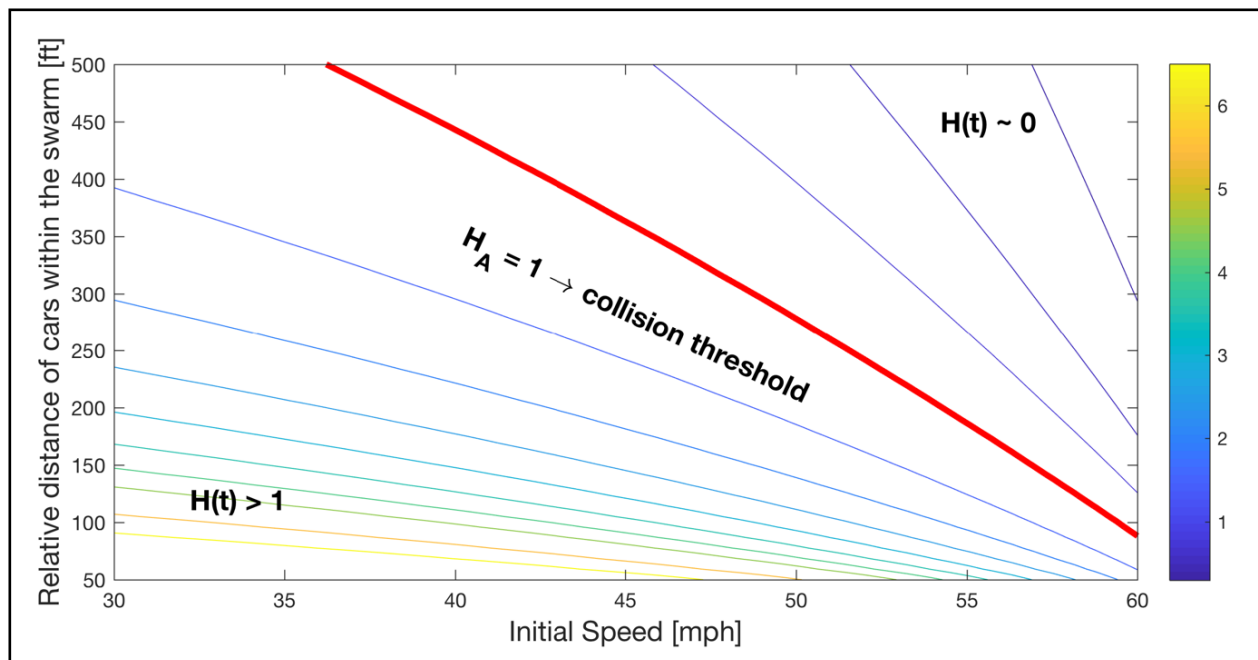


**Figure 27. Speed Matching Hazard Level for Vehicle Entering a Swarm**

Note: Target average speed used is 65 mph with a safety margin of one second.

The previous analysis can be used to optimize and design the parameters of the swarm in terms of relative distance, speed, and safety margins. In combinations with the rules of collision avoidance and minimization of the angular and lateral error, an optimization problem can be set up to ensure things like traffic smoothness, or that a large number of vehicles is allowed in the swarm. These avenues are left as options for future work now that feasibility of the rules of the control-triggering hazard functions has been proven in this preliminary study.

## IV. CONCLUSIONS

### PUTTING IT ALL TOGETHER

This report presented the results obtained from a feasibility study on the adaptation of the concept of particle swarm to monitor the operational status of families of autonomous vehicles from a system safety perspective. Particle swarm motion has been recently brought to the attention of the research community for setting up control frameworks in relation to autonomous vehicles (Fredette and Özgüner, 2017). While the original application of particle swarm was within mathematical optimization (Kennedy and Eberhart, 1995), it was later employed for simulation of multi-agent systems for both animated and inanimate objects, and subsequently researched in the realm of traffic networks simulation (Liu, Passino and Polycarpou, 2003; Suzuki and Yamashita, 1999). The investigators started by modifying some of the particle swarm rules, formulating a framework to monitor the swarm behavior based on laws for collision avoidance, heading selection, and velocity matching to maintain the ongoing motion of the vehicles. To this end, the notion of hazard level and safety thresholds was brought up to define triggers for changes within the actual control inputs available in the autonomous vehicle: steering and acceleration/deceleration. Several different hazard-level functions were preliminarily investigated in this work with the goal of setting up diagnostic tools and establishing safety thresholds to trigger changes in the heading and speed of the vehicles in the swarm. Moreover, some of the explored hazard-level functions had the role of setting up an optimization problem to better define optimal values of relative distance among the cars as well as optimal target speed. The investigated hazard levels, their uses and applicability are summarized in Table 1. Finally, Figure 28 presents a schematic diagram of how each of the proposed functions is interconnected and can work in a process flow to set up the swarm.

**Table 1. Summary of the Developed Functions**

Function	Notes	Uses
$H(t) = \frac{d_{stop_A}(t)}{d_B(t) - d_A(t)}$	1-D stopping distance along the longitudinal axis to ensure sufficient separation	Reset of swarm target velocity (module/value only) and relative distance 1-D steady condition
$H_{ij}(t) = \frac{\varepsilon_i + \varepsilon_j}{\ \vec{d}_i - \vec{d}_j\ }$	2-D collision avoidance through spheres of influence to ensure separation and cohesion	Reset of swarm target velocity and relative distance 2-D steady condition
$H(t) = \frac{e_L + v(t)t \sin e_\theta}{\frac{w}{2}}$	Angular and lateral error function to avoid lane departure/collision with dividers	Computation of maximum time of refresh for recomputation of steering and acceleration/braking inputs
$H(t) = \frac{SM_{time} + t_{acceleration}}{t_{passby}}$	Comparison of time for incoming vehicle to match velocity of the swarm while avoiding collision with safety margin	Transitory situation of vehicle entering the swarm—reset of target velocity and relative distance in transient condition

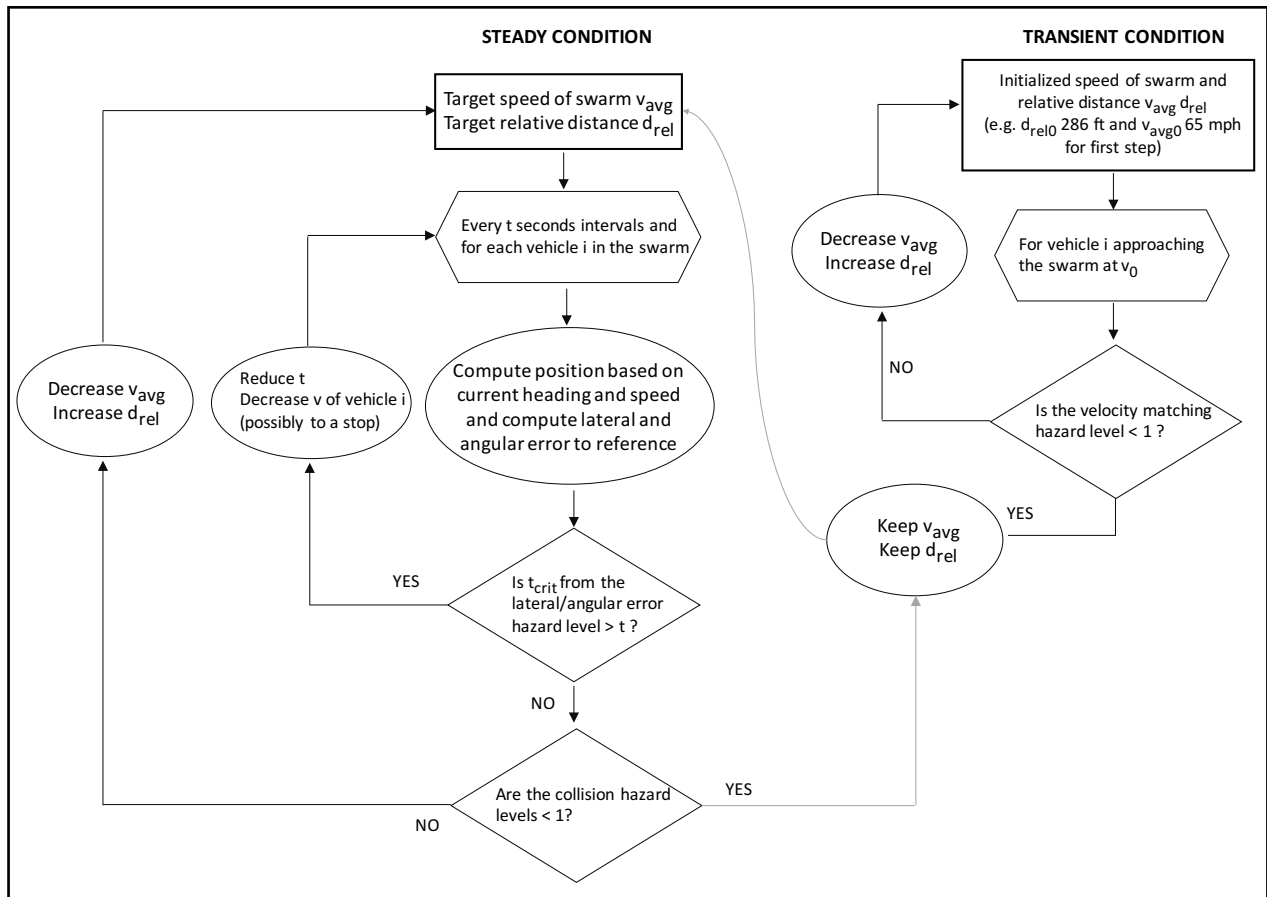


Figure 28. Flow Diagram for the Application of the Proposed Concepts

## FUTURE WORK AND EXTENSIONS

All the analyses presented were preliminary in nature, and employed simple models for the vehicle dynamics. Several extensions of the present work were highlighted and can be summarized as follows:

1. Enhancement of the vehicles dynamic models: refinement of the equations of motion for the vehicle is the first venue for future refinements of the work. Air resistance, traction details, axle geometry, and braking efficiency are a few factors that can improve the current model. The modeling of those aspects was beyond the current proof-of-concept work, which employed a simple rigid-body model for the whole vehicle, with no lateral slip.
2. Enhancement of the spheres of influence: the notion of sphere of influence should be replaced by boxes with geometry depending on the specific vehicles in use. The argumentation behind the 2-D collision avoidance hazard level thus is a simplification of a more complex geometric formatting that would need to be explored.

3. Full family simulation: in this report we investigated relations with up to three vehicles. All the equations presented are still applicable to the N-vehicles problem, but more involved simulations would be needed to analyze those cases. Once more, the presented work only showed feasibility and not detailed results for the full family of vehicles.
4. Optimization of parameters: as highlighted in the work, the hazard-level functions can be periodically and iteratively reassessed, and the parameters of interest for relative distance/swarm geometry, target speed, and safety margins employed can all be optimized. This is an important future avenue of research.
5. Refinement of mode of operations for cluster definition: this report investigated only the steady state and the transient-vehicle entrance mode for the cluster definition. The problem of vehicles exiting the swarm is only preliminarily addressed by the distance threshold from the centroid of the swarm, but more careful analysis of the problem will need to be studied for on-road implementation. Moreover, the emergency and idle modes are also left for future work.

We believe that the concluded research shows promise of integration within autonomous vehicles for the development of artificial intelligence algorithms. This approach can serve as backup to more traditional deep learning algorithms currently in use. Indeed, one of the motivations behind this study came from the need to balance the reliance of autonomous technology on machine learning approaches. Currently, AV technology leverages information from a host of sensors and input channels that allow the car to gather information regarding the surrounding environment. Machine learning algorithms are then responsible for giving the vehicle an actual “brain” and enabling the vehicle to make sense of the data (e.g., “understand” that a moving series of dots is a person, or that a traffic light is turning red, or that a road sign warns of a detour ahead). In some situations, it is possible to foresee that sensors’ malfunctions or the need for additional training of the algorithm may leave the vehicle “lost” and incapable of making a decision about what movement to execute next (e.g., misclassification of an obstacle, or lost feed from lane markings). This is when approaches like the one explored in this work can become useful. The implementation of the particle swarm rules within the vehicle’s brain can be thought of as an additional piece of artificial intelligence embedded in the vehicle that can increase the overall reliability of a family of vehicles, provided that one of them is still capable of recognizing the surrounding environment.

In order to prove such integration, a first step would be the simulation of an entire family of vehicles, to understand how the interaction of multiple entities monitoring the same hazard-level functions would unfold. This first investigation could potentially lead to changes within both the vehicle cluster definition, as well as the particular hazard levels to monitor for each vehicle. Moreover, further steps for future research would involve the integration of the proposed rules with traditional machine learning approaches, and a check from a reliability standpoint of how much the overall functionality of the vehicles improves.

---

## ACRONYMS AND ABBREVIATIONS

---

ACC	Adaptive Cruise Control
AV	Autonomous Vehicle
DoT	Department of Transportation
IDW	Inverse Distance Weights
MTI	Mineta Transportation Institute
PID	Proportional Integral Derivative
PSO	Particle Swarm Optimization
V2V	Vehicle to Vehicle (communication)

---

---

## BIBLIOGRAPHY

- Allouche, Yair, and Michael Segal. 2015. "Cluster-Based Beacons Process for VANET." *Vehicular Communications* 2(2): 80-94.
- Åsljung, Daniel, Jonas Nilsson, and Jonas Fredriksson. 2017. "Using Extreme Value Theory for Vehicle Level Safety Validation and Implications for Autonomous Vehicles." *IEEE Transactions on Intelligent Vehicles* 2(4): 288-297.
- Barnes, Laura, MaryAnne Fields, and Kimon Valavanis. 2007. "Unmanned Ground Vehicle Swarm Formation Control Using Potential Fields." In *Proceedings of the 15<sup>th</sup> Mediterranean Conference on Control & Automation*, Athens, Greece, July 27-29, 2007: 1-8.
- Bidoki, Mohsen, Mehdi Mortazavi, and Mehdi Sabzehparvar. 2018. "A New Approach in System and Tactic Design Optimization of an Autonomous Underwater Vehicle by Using Multidisciplinary Design Optimization." *Ocean Engineering* 147: 517-530.
- Burmeister, Birgit, Afsaneh Haddadi, and Guido Matylis. 1997. "Application of Multi-Agent Systems in Traffic and Transportation." *IEE Proceedings-Software* 144(1): 51-60.
- Burrough, Peter A., Rachael A. McDonnell, and Christopher D. Lloyd. 2015. *Principles of Geographical Information Systems*. Oxford: Oxford University Press.
- Cetin, Nurhan, Kai Nagel, Bryan Raney, and Andreas Voellmy. 2002. "Large Scale Multi-Agent Transportation Simulations." *Computer Physics Communications*, 147(1-2): 559-564.
- Chater, N., Misyak, J., Watson, D., Griffiths, N. and Mouzakitis, A., 2018. "Negotiating the Traffic: Can Cognitive Science Help Make Autonomous Vehicles a Reality?" *Trends in Cognitive Sciences* 22(2): 93-95.
- Corner, Joshua J., and Gary B. Lamont. 2004. "Parallel Simulation of UAV Swarm Scenarios." In *Proceedings of the 36th Conference on Winter Simulation*, Washington, DC, December 5-8, 2004: 355-363.
- Favarò, Francesca M., and Joseph H. Saleh. 2016. "Toward Risk Assessment 2.0: Safety Supervisory Control and Model-Based Hazard Monitoring for Risk-Informed Safety Interventions." *Reliability Engineering & System Safety* 152: 316-330.
- Favarò, Francesca M. and Joseph H. Saleh. 2018. "Application of Temporal Logic for Safety Supervisory Control and Model-Based Hazard Monitoring." *Reliability Engineering & System Safety* 169: 166-178.

- 
- Fredette, Danielle, and Ümit Özgüner. 2017. "Swarm-Inspired Modeling of a Highway System with Stability Analysis." *IEEE Transactions on Intelligent Transportation Systems* 18(6): 1371-1379.
- Hunaini, Fachrudin, Imam Robandi, and Nyoman Sutantra. 2016. "Optimization of Automatic Steering Control on a Vehicle with a Steer-by-Wire System Using Particle Swarm Optimization." *Turkish Journal of Electrical Engineering & Computer Sciences* 24(2): 541-557.
- Kennedy, James, and Russel Eberhart. "Particle Swarm Optimization." In *Proceedings, IEEE International Conference on Neural Networks, IV*, Piscataway, New Jersey, 1995: 1942-1948.
- Kurtze, Douglas A. and Daniel C. Hong. 1995. "Traffic Jams, Granular Flow, and Soliton Selection." *Physical Review E* 52(1): 218.
- Li, Perry Y. and Ankur Shrivastava. 2002. "Traffic Flow Stability Induced by Constant Time Headway Policy for Adaptive Cruise Control Vehicles." *Transportation Research Part C: Emerging Technologies* 10(4): 275-301.
- Liu, Yang, Kevin M. Passino, and Marios M. Polycarpou. 2003. "Stability Analysis of M-Dimensional Asynchronous Swarms with a Fixed Communication Topology." *IEEE Transactions on Automatic Control* 48(1): 76-95.
- Malakorn, Kristin J., and Byunkyu Park. 2010. Assessment of Mobility, Energy, and Environment Impacts of IntelliDrive-Based Cooperative Adaptive Cruise Control and Intelligent Traffic Signal Control. In *Proceedings of the 2010 IEEE International Symposium on Sustainable Systems and Technology (ISSST)*, Arlington, Virginia, USA, May 17-19, 2010: 1-6.
- Mehar, Arpan, Satish Chandra, and Senathipathi Velmurugan. 2013. "Speed and Acceleration Characteristics of Different Types of Vehicles on Multi-Lane Highways." *European Transport* 55: 1825-3997.
- Moussaid, Mehdi, Simon Garnier, Guy Theraulaz, and Dirk Helbing. 2009. "Collective information processing and pattern formation in swarms, flocks, and crowds." *Topics in Cognitive Science*. 1(3):469-97.
- Nowakowski, Christopher, Jessica O'Connell, Steven E. Shladover, and Delphine Cody. 2010. "Cooperative Adaptive Cruise Control: Driver Acceptance of Following Gap Settings Less than One Second." In *Proceedings of the Human Factors and Ergonomics Society Annual Meeting*, Los Angeles, CA, USA, September, 2010, 54 (24): 2033-2037.
- Özkul, Mükremin, and Ilir Çapuni. 2014. "An Autonomous Driving Framework with Self-Configurable Vehicle Clusters." In *2014 International Conference on Connected Vehicles and Expo (ICCVE)*, Vienna, Austria, November 3-7, 2014, 463-468.

- 
- Ploeg, Jeroen, Bart T. M. Scheepers, Ellen Van Nunen, Nathan Van De Wouw, and Henk Nijmeijer. "Design and Experimental Evaluation of Cooperative Adaptive Cruise Control." *2011 14th International IEEE Conference on Intelligent Transportation Systems (ITSC)*, Washington, DC, USA, October 5-7, 2011. doi:10.1109/itsc.2011.6082981.
- Reynolds, Craig. "Flocks, Herds and Schools: A Distributed Behavioral Model." *1987 Proceedings of the 14th Annual Conference on Computer Graphics and Interactive Techniques* 21(4): 25-34.
- Saleh, Joseph H., Rachel A. Haga, Francesca M. Favarò, and Efstathios Bakolas. 2014. "Texas City Refinery Accident: Case Study in Breakdown of Defense-in-Depth and Violation of the Safety–Diagnosability Principle in Design." *Engineering Failure Analysis* 36: 121-133.
- Shi, Yuhui, and Russell C. Eberhart. "Empirical Study of Particle Swarm Optimization." In *Proceedings of the 1999 Congress on Evolutionary Computation*, Washington, DC, USA, July 6-9, 1999. 3: 1945-950.
- Suzuki, Ichiro, and Masafumi Yamashita. 1999. "Distributed Anonymous Mobile Robots: Formation of Geometric Patterns." *SIAM Journal on Computing* 28(4): 1347-1363.

## **PEER REVIEW**

San José State University, of the California State University system, and the MTI Board of Trustees have agreed upon a peer review process required for all research published by MTI. The purpose of the review process is to ensure that the results presented are based upon a professionally acceptable research protocol.

Research projects begin with the approval of a scope of work by the sponsoring entities, with in-process reviews by the MTI Research Director and the Research Associated Policy Oversight Committee (RAPOC). Review of the draft research product is conducted by the Research Committee of the Board of Trustees and may include invited critiques from other professionals in the subject field. The review is based on the professional propriety of the research methodology.

# MTI FOUNDER

Hon. Norman Y. Mineta

## MTI BOARD OF TRUSTEES

### Founder, Honorable Norman Mineta (Ex-Officio)

Secretary (ret.), US Department of Transportation  
Vice Chair  
Hill & Knowlton, Inc.

### Honorary Chair, Honorable Bill Shuster (Ex-Officio)

Chair  
House Transportation and Infrastructure Committee  
United States House of Representatives

### Honorary Co-Chair, Honorable Peter DeFazio (Ex-Officio)

Vice Chair  
House Transportation and Infrastructure Committee  
United States House of Representatives

### Chair, Grace Crunican (TE 2019)

General Manager  
Bay Area Rapid Transit District (BART)

### Vice Chair, Abbas Mohaddes (TE 2018)

President & COO  
Econolite Group Inc.

### Executive Director, Karen Philbrick, PhD (Ex-Officio)

Mineta Transportation Institute  
San José State University

### Richard Anderson (Ex-Officio)

President and CEO  
Amtrak

### Laurie Berman (Ex-Officio)

Director  
California Department of Transportation

### Donna DeMartino (TE 2018)

General Manager and CEO  
San Joaquin Regional Transit District

### Mortimer Downey\* (TE 2018)

President  
Mort Downey Consulting, LLC

### Nuria Fernandez\* (TE 2020)

General Manager & CEO  
Santa Clara Valley Transportation Authority

### John Flaherty (TE 2020)

Senior Fellow  
Silicon Valley American Leadership Forum

### Rose Guilbault (TE 2020)

Board Member  
Peninsula Corridor Joint Powers Board

### Ed Hamberger (Ex-Officio)

President & CEO  
Association of American Railroads

### Steve Heminger\* (TE 2018)

Executive Director  
Metropolitan Transportation Commission (MTC)

### Diane Woodend Jones (TE 2019)

Principal & Chair of Board  
Lea + Elliot, Inc.

### Will Kempton (TE 2019)

Retired

### Art Leahy (TE 2018)

CEO  
Metrolink

### Jean-Pierre Loubinoux (Ex-Officio)

Director General  
International Union of Railways (UIC)

### Bradley Mims (TE 2020)

President & CEO  
Conference of Minority Transportation Officials (COMTO)

### Jeff Morales (TE 2019)

Managing Principal  
InfraStrategies, LLC

### Dan Moshavi, PhD (Ex-Officio)

Dean  
Lucas College and Graduate School of Business  
San José State University

### Dan Smith (TE 2020)

President  
Capstone Financial Group, Inc.

### Paul Skoutelas (Ex-Officio)

President & CEO  
American Public Transportation Authority (APTA)

### Beverley Swaim-Staley (TE 2019)

President  
Union Station Redevelopment Corporation

### Larry Willis (Ex-Officio)

President  
Transportation Trades Dept., AFL-CIO

### Bud Wright (Ex-Officio)

Executive Director  
American Association of State Highway and Transportation Officials (AASHTO)

(TE) = Term Expiration

\* = Past Chair, Board of Trustees

## Directors

### Karen Philbrick, PhD

Executive Director

### Asha Weinstein Agrawal, PhD

Education Director  
National Transportation Finance Center Director

### Hilary Nixon, PhD

Research & Technology Transfer Director

### Brian Michael Jenkins

National Transportation Security Center Director

## Research Associates Policy Oversight Committee

### Jan Botha, PhD

Civil & Environmental Engineering  
San José State University

### Katherine Kao Cushing, PhD

Environmental Science  
San José State University

### Dave Czerwinski, PhD

Marketing and Decision Science  
San José State University

### Frances Edwards, PhD

Political Science  
San José State University

### Taeho Park, PhD

Organization and Management  
San José State University

### Christa Bailey

Martin Luther King, Jr. Library  
San José State University



